TECHNICAL REPORT STANDARD PAGE

1. Report No.	2. Government Accession No.	3. Recipient's Catalog No.
FHWA/LA-02/345		

4. Title and Subtitle	5. Report Date
Evaluation of Modified Asphalt Using Chlorinated and Maleated Waste Polymers	July 2002
	6. Performing Organization Code

7. Author(s)	8. Performing Organization Report No.
William H. Daly, Ioan I. Negulescu, Pei-Hung Yeh, Louay N. Mohammad	345

9. Performing Organization Name and Address	10. Work Unit No.
Department of Chemistry, Louisiana State University, Baton Rouge, LA 70803-1804	11. Contract or Grant No. 95-3B

12. Sponsoring Agency Name and Address	13. Type of Report and Period Covered
Louisiana Transportation Research Center 4101 Gourrier Avenue Baton Rouge, LA 70808	Final Report Period Covered: 10/01/95-6/30/98
	14. Sponsoring Agency Code

15. Supplementary Notes

16. Abstract

Asphalt modification using polymeric additives derived from solid wastes, i.e. polyolefins, is reported. Chlorination of polyethylene can be controlled to produce semicrystalline polymeric additives. Differential scanning calorimetry can be used to determine the asphalt crystallinity and the distribution components among phases in asphalt/polymer blends. To enhance the resolution of a given thermogram, a several-step annealing process is required to experimentally realize a near-equilibrium state. Introducing chlorine atoms on polyethylene chains can improve the compatibility of the asphalt/polymer blends by adjusting the interaction between the components of asphalt and polymer. Maleation of polyolefins at very low levels (one to two percent) is an effective means for enhancing the polarity of the additive without influencing the degree of crystallization. The more polar additives also produce compatible polymer/asphalt blends. The chlorinated polyethylene-modified hot mix asphalt cement did show improved fundamental engineering properties relative to tank asphalt at all temperatures.

17. Key Words	18. Distribution Statement
Thermal analysis of asphalt and/or asphalt blends chlorinated polyethylene(CPE), maleated polypropylene (MPP), asphalt/CPE or MPP blends, Superpave based grading, dynamic mechanical analysis, TFOT aging, PAV aging, HMAC engineering properties	Unrestricted. This document is available through the National Technical Information Service, Springfield, VA 21161.

19. Security Classif. (of this report)	20. Security Classif. (of this page)	21. No. of P ages	22. Price
None	None	106	N/A

EVALUATION OF MODIFIED ASPHALT USING CHLORINATED AND MALEATED WASTE POLYMERS

by

William H. Daly, Ph.D.
Alumni Professor of Chemistry

Ioan I. Negulescu, Ph.D.
Associate Professor of Chemistry, Research

Pei-Hung Yeh
Graduate Student in Chemistry

Louay N. Mohammad, Ph.D.
Associate Professor of Civil and Environmental Engineering

LTRC Research Project No. 95-3B
LTRC Project No. 345
State Project No. 736-99-0212

Conducted for

Louisiana Department of Transportation and Development
Louisiana Transportation Research Center

In cooperation with

U. S. Department of Transportation
Federal Highway Administration

July 2002

ABSTRACT

Asphalt modification using polymeric additives derived from solid wastes, i.e. polyolefins, is reported. Chlorination of high density polyethylene (HDPE) can be controlled to produce semicrystalline chlorinated polyethylenes (CPE) with two different chlorine contents, 5.8 and 24.5 weight percent. Introducing chlorine atoms on polyethylene chains can improve the compatibility of the asphalt/polymer blends by adjusting the interaction between the components of asphalt and polymer. Environmental scanning electron microscopy shows that the dispersed CPE-rich phase was larger than the HDPE-rich phase in asphalt blends. Maleation of polyolefins at very low levels (one to two percent) is an effective means for enhancing the polarity of the additive without influencing the degree of crystallization. The more polar additives also produce compatible polymer/asphalt blends.

Differential scanning calorimetry (DSC) can be used to determine the asphalt crystallinity and the distribution components among phases in asphalt/polymer blends. To enhance the resolution of a given thermogram, a several-step annealing process is required to experimentally realize a near-equilibrium state. The asphalt thermograms from different sources exhibit distinctly different transitions; the technique may be useful in identifying asphalt sources.

Standard procedures for studying the physical and engineering properties of asphalt binders have been used to specify the pg grading of the blends according to superpave protocols. The polymer/asphalt blends exhibit significantly better properties than those of tank asphalts. The blends exhibit higher viscosity at high temperature, higher rutting resistance, reducing age hardening for long-term temperature cracking, and lower creep stiffness at low-temperature cracking response than tank asphalts.

A study was conducted to examine the feasibility of using waste materials converted to CPE as modifiers to paving grade asphalt. Both a binder rheology study and a mixture characterization were conducted to compare the performance of conventional dense graded mix containing AC-20 and CPE modified AC-20. In general, the addition of CPE has improved the mix properties measured from the indirect tensile strength test, indirect resilient modulus test, indirect creep test, and fatigue test. The binder rheology correlated well with mix properties. The CPE-modified hot mix asphalt concrete did show improved fundamental engineering properties relative to tank asphalt at all temperatures.

IMPLEMENTATION STATEMENT

This study encompassed exploratory work to examine the procedures for producing stable modified polyolefin/asphalt blends by treating the polyolefin with chlorine or maleic anhydride prior to mixing it with asphalt. Currently, there are no directly implementable results. However, the annealing procedure developed should be considered in asphalt thermal analysis. It has been shown that careful thermal pretreatment of an asphalt sample before conducting differential calorimetry scan reveals distinctive thermal transitions. If a set of standards from various asphalt sources is run, the DSC scan can be used to identify the source of an unknown asphalt. Thus, if specifications call for a specific asphalt source, it is possible to confirm that asphalt from that source has been used to prepare the polymer modified asphalt cement (PMAC).

TABLE OF CONTENTS

LIST OF TABLES

LIST OF FIGURES

LIST OF SCHEMES

INTRODUCTION

Since the advent of asphalt paving blocks in 1824, efforts to improve the properties of asphalt surfacing materials have centered on polymeric additives. In the 1840's, patents describing the modification of bitumen with gutta percha or natural rubber appeared, and, as each new polymer was developed, its potential interaction with asphalt was evaluated. Since the addition of polymers increases the cost of the corresponding polymer modified asphalt cement (PMAC), the new material must increase the durability of the mix and meet all climatic requirements without compromise. Indeed, addition of appropriate polymers to asphalt increases fatigue cracking resistance, reduces the extent of permanent deformation, improves thermal cracking resistance, lessens moisture sensitivity, and reduces age hardening. Polymers typically employed in PMAC's include natural rubber latexes, styrene-butadiene latexes, styrene-butadiene-styrene (SBS) thermoplastic rubbers, polyethylene (PE), other polyolefins, and ethylene-vinyl acetate (EVA) copolymers *[1]*. Polyolefins and vulcanized rubber also represent major components of solid wastes; therefore, incorporation of these materials into polymer modified asphalt cements is an effective method of polymer recycling.

Addition of SBS block elastomers to asphalt increase resistances of the resultant PMAC to rutting at warm temperatures and improves the low temperature ductility, elasticity, and cyclic loading properties of the mixture *[2]*. Blends of polymeric materials with asphalt are complex and characteristically unique paving material systems. For any specific asphalt cement (AC), the physical properties of the asphalt/polymer blend are affected by the amount of polymeric material added, its composition, its molecular weight, etc. However, the most important variable is the compatibility of the AC with the admixed polymer. The ability to enhance polymer/asphalt compatibility is complicated further by source dependent variations in asphalt compositions within a given grade. Our research efforts are directed toward enhancing the compatibility of polymer additives with asphalts, assessing the phase structures of the asphalt/additive blends, and comparing the properties of PMAC with those of the pure asphalt matrix.

Molecular structures of asphalt are highly diverse, but three basic structures are generally recognized: straight or branched aliphatic chains, simple and complex naphthenic rings, and heteroaromatic systems *[3]*. Durable asphalts are comprised of these components, interacting to form a balanced, compatible system. The asphaltenes are suspended in the oils

by the resins, making asphalt a colloidal system. An extensive study on the chemistry and physical properties of asphalts has just been completed under the auspices of the Strategic Highway Research Program (SHRP), and new performance-based specifications based upon dynamic testing techniques before and after controlled aging have been proposed *[4]*.

Thermal Characterization of Asphalts

Asphalts are aggregates rather than homogeneous systems and, thus, undergo a solid/liquid transition, which involves both an amorphous phase and a crystalline phase. The impact of crystallized fractions in asphalt and crude oil on physical and rheological properties of asphalt is well documented. Differential scanning calorimetry (DSC) has proved to be a very useful technique for estimating both the crystalline fraction and the glass transition temperature of asphalt samples. Further, changes in these features provide a sensitive method for assessing asphalt/polymer blend compatibility *[5]*.

F. Noel and L. W. Corbett obtained DSC thermographs of asphalts over a broad range of temperatures, enunciated a need to establish a consistent thermal history prior to comparing different asphalts, and quantified the crystalline components *[6]*. Blanchard et. al described techniques for measuring glass transition (Tg) temperatures of asphalt fractions *[7]*, while Claudy et. al devoted great efforts to studying the crystallized fraction in asphalt *[8], [9], [10]*. Their research shows that the endothermic transitions in the DSC thermogram stems from the melting/dissolution of crystallized molecules in the saturated fraction of asphalt. In the initial phases of this work, we developed an analytic method that combines careful annealing protocol with DSC to identify asphalt sources *[5]*. We have applied this procedure to the characterization of standard asphalts, asphalts employed in Louisiana, and all of the polymer/asphalt blends.

Compatibility of Polymer Additives with Asphalt

The introduction of any incompatible polymer under agitation into such a system at high temperature generally results in asphaltene flocculation and oil bleeding, leading to a binder without cohesion *[11]*. Even if the phase separation of the asphalt components is not apparent, extended mixing times will be required to achieve acceptable mixes *[12]*. Polymers must improve not only AC properties, but must improve the performance of a binder/aggregate combination as well *[13]*. Studies on the application of Superpave PG procedures to those of PMAC indicate that the long term behavior of PMAC mixes can also be predicted by dynamic rheological tests *[2]*.

Plastics give strength to the asphalt, but the ability to recover from extension is lost *[14]*. Thermoplastics, which are partially crystalline such as PE and polypropylene (PP), have attracted more and more attention since this class of polymer combines the advantages of rubber and fibers. The crystalline segments of polyolefins serve as high strength fillers in the asphalt/polymer blend and improve the blend properties over all service conditions. However, the polyolefins are only slightly compatible with asphalt; thus, the blends tend to separate at high temperatures. Ethylene-vinyl acetate (EVA) copolymers are more compatible and improve resistance to permanent deformation and increase modulus. The presence of vinyl acetate comonomers decreases the crystallinity of the PE blocks, leading to increased flexibility and toughness. In one study on surface dressings, the EVA modified asphalt ranked among the best of the asphalts tested in the areas of fatigue resistance and field performance *[15]*. Unfortunately, the properties of EVA blends may vary substantially depending upon the asphalt used to prepare the PMAC, and unsatisfactory mixes can be produced.

Polymer additives should reduce the temperature sensitivity of AC by increasing the high temperature viscosity. Ideally, the resultant binder should have a very low thermal sensitivity throughout the utilization range but a low viscosity at mixing temperatures *[11]*. Resistance to permanent deformation as well as tensile and fatigue strength should be enhanced relative to the properties of the unmodified asphalt. However, the binder must maintain good adhesive properties and exhibit high aging resistance. A suitably prepared PMAC should exhibit reduced plastic deformation at high temperatures, better low temperature resiliency, and better performance in service under heavy oscillatory loads.

Utilization of Modified Polyolefins

If price and availability of various polymers that have been proposed for asphalt modification are considered, it is obvious that PE or waste polyolefins would be more economical than other polymeric candidates. Further, since polyolefins comprise approximately 60 percent of plastic solid wastes, a reliable source of polyolefins, either from virgin material or from recycled waste, is assured. Polyethylene is a potentially useful modifier for increasing the low temperature fracture toughness of asphalt concrete *[16]*, and it may confer additional pavement stability at elevated temperatures, which would minimize rutting and distortion due to creep. High density linear polyethylene is highly crystalline but the amorphous domain exhibits a very low glass transition temperature. This allows polyethylene to contribute additional toughness and ductility at low temperatures to PE/asphalt blends, particularly those prepared from soft asphalts. However, it is known that asphalt/polyethylene mixtures

have a tendency toward gross phase separation, i.e., gross incompatibility, when standing at elevated temperatures for long periods *[17]*. Therefore, modification of PE is needed to enhance its compatibility with asphalt.

Modification of PE by chlorination is a simple technique to change the polarity, to reduce the crystallinity, and to increase the elasticity of the polymer. Partially chlorinated polyolefin waxes were reported to improve stability of asphalt/polymer blends *[18]*, *[19]*, so PE with various degrees of chlorination to improve the polymer interaction with polar components of asphalt were prepared and characterized. The extent of chlorination can be used to vary the crystallinity of the polymer additive. The crystalline domains of polyolefins contribute to high temperature reinforcement while their amorphous domains, which exhibit very low Tg temperatures, contribute additional toughness and ductility at low temperatures to polyolefin/asphalt blends, particularly those prepared from soft asphalts.

Maleation of Polyolefins

Grafting of reagents to preformed polymers is an important method for preparing polymers with reactive functional groups. The addition of maleic anhydride (MAH) to ethylene was chosen because the reaction can be conducted by simply using reactive extrusion on a variety of polyolefins *[20]* and because a reasonable level of substitution (1-3 weight percent) can be achieved. The modified polymer consists of a polyolefin backbone with pendent succinnic anhydride (SAH) functional groups. The pendent anhydride moieties provide functionality for cross-linking and further chemical modification.

Polyolefins can be modified by maleation to introduce some desirable properties into the polymer without adversely affecting the nature of polymer chain. Maleic anhydride can be grafted onto the polyolefins in a solution *[21]* or in the melt *[22]*. An overview of this chemistry is provided by Singh *[23]*. The initiation of the grafting can be either by peroxide decomposition or by thermal/mechanical radical formation. In general, modifications of polyolefins have improved adhesion to metals, glass fibers, wood fibers, and other polymers *[24]*. One would expect similar favorable interaction with the polar components of asphalts.

The modification of polyolefins with MAH by reactive processing in an extruder is of particular interest. Evaluation of maleation of PP through reactive extrusion process, taking into consideration the energy balance and environment conservation, indicates that the process could be employed in polyolefin recycling. Carraher and Moore *[25]* reported the reaction of MAH with polyolefins in the presence of a peroxide initiator generally results in

grafting of MAH to the polyolefin backbone, but the reaction is accompanied by crosslinking or polymer chain scission. These side reactions are due to a generation of backbone chain radicals followed by coupling or disproportionation *[20]*. However, Gaylord *[26]* reported that the presence of low or high molecular weight compounds containing nitrogen, sulfur, or phosphorous atoms can reduce or prevent these kinds of undesirable reactions.

The addition of maleic anhydride to PP was chosen for this work because the reaction can be conducted by simply using reactive extrusion and a reasonable level of substitution (two to three weight per cent) can be achieved. The modified polymer consists of a polymer backbone with pendant SAH functional groups. Products containing up to 2.5 weight per cent MAH, which appears to be the maximum concentration compatible with asphalt, can be synthesized from PP. The pendent anhydride moieties provide functionality for cross-linking and further chemical modification, i.e., the subsequent reactions accomplished by the addition of polyvinyl alcohol (PVA), various amines, etc. A commercial extrusion process for MAH grafted PP is currently being run at the Adell Plastics plant in Denham Springs, Louisiana.

In a preliminary study, grafting of MAH to PE was effected in a solution and molten PE, in the presence of free radical initiators *[27]*. Conditions, which minimize the cross-linking of PE, were developed and techniques for characterizing the products using NMR, FTIR, and DSC were calibrated. These techniques are applied to the characterization and further modification of commercial maleated PP in this study.

Asphalt/Polymer Blends

Blends of high density polyethylene, chlorinated polyethylene, and maleated polypropylene were prepared with asphalt typically employed in Louisiana. These blends have been evaluated using Superpave PG protocols including: high temperature viscosity measurement, dynamic mechanical analysis (DMA), and bending beam tests. Differential scanning calorimetry (DSC), fluorescence reflection microscopy and FTIR were also employed to characterize PMAC's. In addition, creep resistance and low temperature crack resistance of the asphalt and the PMAC's were evaluated. The results confirm that CPEs with up to 24.5 weight percent Cl are more compatible with asphalt than HDPE. Marked improvements in blend properties are also observed with maleated PP, provided that the degree of maleation does not exceed 3 percent.

Asphalt cement, mixed with aggregate, forms hot mix asphalt cement concrete mixes. Polymer modified asphalt cements exhibit enhanced pavement performance with decreasing temperature susceptibility and increasing resistance to permanent deformation and load-associated cracking *[28], [29]*. This report describes the results of a laboratory study of the potential use of CPE as a modifier in asphalt concrete mixes. The goal of this study was to evaluate chemically modified polymer additives introduced to enhance the rheological properties of asphalt binders and to establish engineering properties in both static and dynamic modes for HMAC.

OBJECTIVES AND SCOPE

The goal of this study was to identify the extent of polyolefin modification needed to optimize the properties of asphalt binders containing the polyolefin component of solid wastes. The best binder combination was selected to prepare asphalt cements. The properties of these cements were compared with typical commercial polymer modified concrete with respect to performance.

The special goals were:

1. To prepare a series of CPE (chlorinated polyethylene) blends with AC-10, AC-20 and AC-30 asphalt cements used in Louisiana and assess the stability of each blend.
2. To evaluate the potential for using DSC to identify asphalt sources.
3. To evaluate the potential for using DSC to assess asphalt/polymer blend compatibility
4. To conduct binder rheology studies on CPE/asphalt blends according to Superpave PG protocols.
5. To conduct a mixture characterization study comparing the performance of conventional dense graded mix containing tank ACL-2 (conventional AC 20 from Lion Oil Company) and CPE modified ACL-2.

Asphalt from four Louisiana refineries was used to prepare blends of modifiers with AC-10, AC-20, and AC-30 asphalt cements. The additive level was set at three weight percent and only two CPEs (5.8 weight percent Cl and 24.5 weight percent Cl) were examined. Only a commercially available MPP was studied in detail, but procedures for preparing maleated polyolefins in general were developed. A single blending condition, i.e., adding the polymer to asphalt under vigorous stirring at 150°C and blending for 40 minutes, was employed. Samples for DSC analysis were subjected to an annealing protocol that enhanced the magnitude and distinctiveness of the thermal transitions. All samples were characterized by DSC; the tank asphalt source and the polymer blend interaction were identified.

Dynamic mechanical testing procedures were employed to characterize all polymer/asphalt blends. All tank asphalts and blends were subjected to aging by TFOT, followed by PAV, and graded using Superpave PG procedures. Low temperature creep response at -12°C was determined on the all samples with bending beam rheometry (BBR).

A blend of CPE (24.5 weight percent Cl) with ACL-2 that exhibited the best binder properties was selected to prepare an HMAC. It was based upon a dense graded aggregate mix according to the specification criteria for a type 3 binder course. The mix properties were measured using a Materials Test System (MTS 810). Indirect tensile strength (ITS) and strain, indirect tensile resilient modulus (M_R), indirect tensile creep, and fatigue tests were performed on standard asphalt briquettes.

METHODOLOGY

Preparation and Characterization of Materials

Polymer modified asphalts were prepared using AC-10, AC-20, or AC-30 grade materials, which were obtained from the Louisiana Transportation Research Center (LTRC). Polymers investigated as asphalt additives were HDPE, which was supplied by Paxon Polymer Company, maleated polypropylene supplied by Adell Plastics and chlorinated polyethylene, prepared as described below.

Preparation of Chlorinated Polyethylenes

HDPE, weight, and number average molecular weights of 8.5×10^4 and 1.9×10^4 doltons, respectively, was chlorinated to produce two different CPE's, a semi-crystalline material with a chlorine content of approximately 6 weight percent and an amorphous material containing 24.5 weight percent chlorine. In a typical solution chlorination, 105 g of the HDPE power was placed in a four-neck reaction flask with 1000 ml of 1,1,2,2-tetrachloroethane (TCE). The vessel was equipped with adapters for a nitrogen and chlorine inlet. The solution was then heated to 115°C and vigorously stirred until the PE dissolved. A constant flow of chlorine gas was introduced to the reactor for periods ranging from two to six hours, depending upon the degree of chlorination desired. The product was isolated by quenching the reaction mixture in methanol, washing several times with methanol, and vacuum drying at 55°C for a week. The chlorine content was determined with proton NMR, using a Bruker/AM 400 MHz spectrometer. The samples for ^{1}HNMR analysis were run as 15 percent or 1.5 percent (w/v) solution in para-dichlorobenzene at 115°C to ensure that the entire sample was dissolved.

Preparation of Maleated-Polyethylene: Solution Process

The maleation was conducted using conditions described by Gaylord *[30]*. Low density polyethylene (LDPE), 20 g, Melt Index (MI) = 0.22, was dissolved in 150 ml dichlorobenzene (DCB) at 130°C, and a mixture of 4 g of MAH and 0.68 g triethyl phosphate (TEPA) was added. After raising the reaction temperature to 150°C, the maleation was initiated by adding 1 ml dicumyl peroxide (DCP) solution (0.5 g DCP in 15 ml DCB); an additional 1 ml aliquots of DCP solution was injected every 15 minutes. The MAH content was controlled by reaction time. The polymer used in this study was allowed to react for one

hour; the resultant MAH content was 2.8 weight percent. At the end of the reaction, the solution was allowed to cool to room temperature and poured into 750-1000 ml methanol; the precipitate was washed several times with methanol and dried *in vacuo* at room temperature for more than 72 hours.

Calibration Curves for Maleic Anhydride (MAH) Grafting Level

The reaction of maleic anhydride with PP introduces succinic anhydride substituents. The amount of MAH grafting level on PP was determined by a calibration curve, which correlated the quantity of SAH intimately blended with PP with a carbonyl index (CI) calculated from FTIR spectroscopy measurements *[31], [32], [33]*. The carbonyl index was defined as the intensity of the carbonyl peak at 1785 cm^{-1} divided by that of the CH_3 peak at 1165 cm^{-1}. The solutions for determination of SAH grafted polypropylene were prepared by dissolving known amounts of SAH and PP in hot xylene, placing several drops of this solution on KBr plates, and then evaporating the solvent to form thin films. The infrared spectra was measured and the CI calculated. The data yielded the Beer's law calibration plot shown in figure 1. Comparable curves prepared by mixing the appropriate N-substituted succinimide with PP were used to estimate the extent of amine reaction with the MPP.

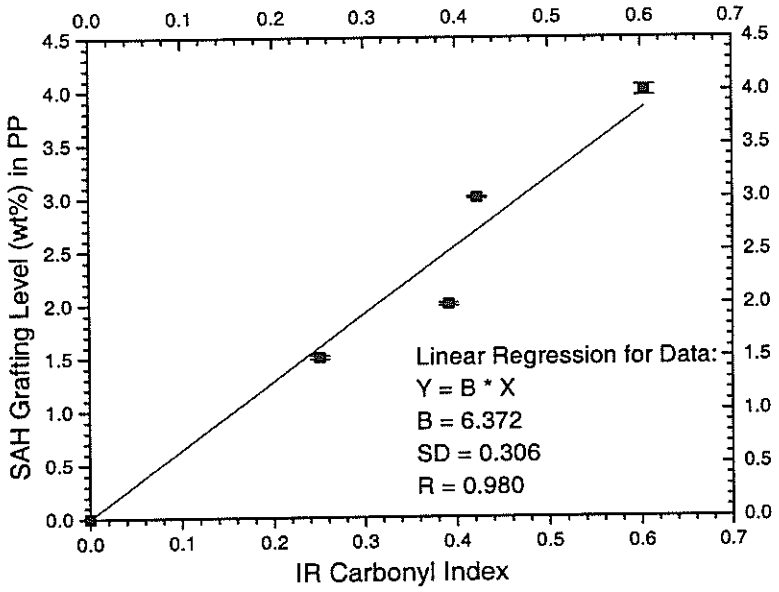

Figure 1
Blends of succinic anhydride with PP vs. FTIR carbonyl index

Modification of Maleated Polypropylene (MPP) with Polyvinyl alcohol (PVA) (MPPPVA)

In a typical solution process, the modification of commercial MPP with PVA was carried out in three, 250 ml, neck round-bottom flasks equipped with stir bar, condensor, thermometer, and an argon gas inlet. A known amount of MPP (10 percent w/v) was dissolved in tetrachloroethylene by heating at 90°C for 24 hours. To this homogenized solution, 1 g of polyvinyl alcohol was added, and the solution was refluxed for four hours. After refluxing, the reaction mixture was then poured into 1.5 L of methanol under vigorous stirring. The precipitated polymer was isolated and washed several times with methanol. The products were dried *in vacuo* at room termperature for three days.

Modification of Maleated Polypropylene (MPP) with Ethanolamine, 1-Naphthylamine and N-aminomorpholine

A MPP solution was prepared from 5 g of MPP and 120 ml of xylene. Ethanolamine, 1-naphthylamine, or N-aminomorpholine (approximately 0.5 g) was added to the reaction flask which contained the solution of MPP. The mixture was refluxed with a gas inlet for four hours. In each case quenching the reaction mixture in methanol, vacuum filtering, and washing several times with methanol was used to isolate the product. Finally, products were dried under reduced pressure at room temperature for three days. The products were designated as follows: maleimide from the reaction of ethanolamine, MPPEA; maleimide from the reaction of 1-naphthylamine, MPPNA; and the maleimide from the reaction of N-aminomorpholine, MPPAM.

In a typical reactive melt process, the modification of MPP with ethanol amine was carried out in a Miniaturized Internal Mixer (MIM), equipped with a torque rheometer (Haake Rheocord 90). The MIM has two rotors that rotate within a chamber to cause a shearing action on the material. After operating for five minutes at 165°C and 60 rpm, 50 g of MPP were added to the mixer and allowed to melt for an additional five minutes before 5 g of ethanol amine was added; the reactants were allowed to mix for five minutes. The total reaction was completed in 15 minutes. Disassembling the mold and scraping the cooling material from the mixer surfaces yielded the product.

Asphalt blending methods

The asphalt (AC-10, AC-20 or AC-30) was heated to 150°C, stirred vigorously while the polymer additive was introduced, and then stirred at 150°C for 40 minutes. A conventional viscosity graded AC-20 (designated as ACL-2) from the asphalt producer, Lion Oil Company, and a CPE modified ACL-2 were used to prepare the asphalt cements used in this study. The modified asphalt was prepared by adding a three weight percent of CPE to the ACL-2 binder. The ACL-2 and CPE modified ACL-2 blends were characterized by SHRP standard procedures to determine binder rheological properties. Table 1 presents the binder properties along the Superpave PG grading criteria.

Hot Mix Aspahlt Mixture (HMA)

The HMA mix needed to be a dense graded mix of limestone and coarse and fine sands to meet the 1992 Louisiana Department of Transportation and Development (DOTD) specification criteria for a type 3 Binder Course (BC) mix. CPE-modified ACL-2 and tank ACL-2 asphalt cements were used in the HMAC for this study. The aggregate source, which was obtained from ACME Gravel, in Baywood, Louisiana, was selected from an actual job mix formula (JMF). The aggregate gradation consisted of 75 percent crushed gravel, 10 percent coarse sand, and 15 percent fine sand. The theoretical gravity for the aggregates was 2.638. The job mix formula for the final asphalt concrete mixes is detailed in table 2.

The optimum binder content selected at four percent air voids was determined from standard Marshall mix design and was equal to 5.4 percent, shown in table 2. Specimens were prepared using 75 blows per face of the Marshall hammer. Each specimen was 4 inches in diameter and about 2.5 inches high. The target air void level was four percent (± 0.5 percent). At the target air void level, samples were statistically grouped to have similar mean air void levels. Each test was conducted in triplicate. The following convention is used to designate the two mixes and their air voids in the results reported for the various tests: A20 is a mixture containing ACL-2 asphalt and C20 is a mixture containing CPE-modified ACL-2 asphalt.

Differential Scanning Calorimetry (DSC)

The relative crystallinity of a given asphalt can be measured by DSC *[6], [8]*. A Seiko DSC 220C, calibrated for temperature and enthalpy with indium, was employed to estimate the relative volume of the crystalline phase in each of the asphalt samples. Analyses were

conducted on ≅ 10 mg samples sealed in an aluminum sample pan using an empty aluminum sample with cap as a reference. Each specimen was cooled from room temperature to -140°C, heated from -140°C to 160°C, and then cooled from 160°C to -100°C at the same rate. The glass transition (Tg) temperatures, melting points (Tm), and enthalpy (ΔH_f) of the blend components were determined as previously described *[5]*.

Table 1

Superpave™ binder specification test results for ACL-2 and CPE modified ACL-2 used to prepare asphalt cements

Test	Property	Test Results		Superpave PG Criteria
		ACL-2	CPE Modified ACL-2	
Original Binder				
Flash Point	n/a	-	-	230°C
Rotational Viscosity (Pa·s)	135°C	0.3	0.8	3 Pa·s max.
Dynamic Shear Rheometry (kPa)	G*/sin δ 64°C	2.7	3.2	1.0 kPa min.
	70°C	1.2	1.5	
TFOT Aged Binder				
Mass Loss (%)	n/a	< 1.0	< 1.0	1% max.
Dynamic Shear Rheometry (kPa)	G*/sin δ 64°C	4.2	5.4	2.20 kPa min.
	70°C	1.8	2.6	
PAV Aged Binder				
Dynamic Shear Rheometry (kPa)	G*sin δ & 25°C	1998	1065	5000 kPa max.
	G*sin δ & 28°C	1521	745	
Bending Beam Rheometry (-12°C)	Stiffness	170	127	300 MPa max.
Bending Beam Rheometry (-12°C)	m-value	0.32	0.33	0.300 min.
PG Grading		64-22	70-22	

Environmental Scanning Electron Microscope (ESEM)

Images of asphalt blends were obtained by using an Electronscan ESEM model E-3 with a lanthanum hexaboride electron gun and a high temperature specimen heating system. The ESEM power was 20 Kev, and the magnification ranged up to 2000x. The Electronscan high temperature specimen heating system replaces the regular specimen stage with a heater

assembly. This system enables controlled heating of the specimen while under observation. Before heating, a specimen of asphalt binder was placed in a removable sample holder mounted on the specimen heater assembly (a hot stage) to control and adjust the temperature. Dynamic videotapes of asphalt blend structural change during heating and cooling conditions were observed using a camera connected to the ESEM.

Table 2
Job mix formula of asphalt cements evaluated

Sieve Size mm, (inch)	DOTD Specification	ACL-2 Mix	CPE Modified ACL-2 Mix
	Percent Passing		
12.5 (1/2")	70-100	97%	97%
9.5 (3/8")	60-95	85%	85%
4.75 (No.4)	40-70	58%	58%
2.0 (No.10)	28-50	38%	38%
0.425 (No.40)	14-30	31%	31%
0.180 (No.80)	8.0-20	16%	16%
0.075 (No. 200)	3.0-8.0	11%	11%
Mixture Components	Mixture Types		
%AC	-	5.4	5.4
%Voids	3.0-5.0	4.4	3.9
%VFA	70-80	74	73
%VMA, Min.	14.0	16.6	16.7

Torque Rheometry

The torque rheometer measures viscosity-related torque caused by the resistance of the material to the shearing action of the plasticating process. The mixing process used in this study incorporated a MIM, equipped with a torque rheometer. Using a Haake Rheocord 90, a mixture of 50 g of AC 10 (designated as ACL-1) from the Lion Oil Company with 3 percent CPEB (24.5 weight percent Cl) was blended at 125°C for 60 minutes. The blend was allowed to cool under agitation at 60 rpm to 50°C (120 minutes required), and the total torque experienced by the sample was recorded.

Binder Aging Method

Representative asphalts and modified asphalts were selected for thin film oven testing (TFOT), which serves to simulate the aging of the asphalt binder during mixing and construction operations (short-term). A pressure aging vessel (PAV) was used to simulate binder aging during five to ten years of service life (long-term). All samples for the PAV were prepared using (50 ± 0.5 g material) and were aged in the TFOT oven at 163°C for five hours under a continuous air flow. The TFOT aged samples were submitted to the next aging step in the PAV at 100°C and 2070 kPa for 20 hours.

Rheology Measurements

Viscosity data were collected at 135°C, where asphalt acts almost entirely as a Newtonian fluid, using a rotational viscometer (spindle #27 and 100 rpm). A dynamic shear rheometer (Bohlin CVO) was used for dynamic mechanical analysis of asphalt binders with the stress equal to 150 Pa at a rate of 1.5 Hz. The samples were "sandwiched" between two parallel plates with a diameter of 25 mm at a gap of 1 mm and cooled down to 5°C through one cycle before performing a temperature sweep to 90°C. The reference temperature was taken as 64°C for rutting factors or 25°C for fatigue cracking factors. Under these conditions, the samples were run under a frequency sweep from 0.001 to 30 Hz at 25°C, 40°C, and 60°C to comply with the Superpave PG asphalt binder specifications suitable for the typical hot climate of Louisiana.

A bending beam rheometer (Applied Test System) was used to characterize the low temperature stiffness response of PAV aged tank asphalts and asphalt/polymer blends. The data, which were recorded at six loading times (8, 15, 30, 60, 120, and 240 seconds) for a load on the beam of 100 ± 5 g, allowed the calculation of the creep stiffness, S(t), and the creep rate of the sample under load, m, as the absolute value of the slope of the log creep stiffness versus log loading time curve.

Creep and Recovery Tests

A constant stress creep/creep recovery test was run at 50°C with a Haake rheometer (RheoStress RS150), using a 25 mm parallel plate system with a gap of 0.25 mm. During a first test stage, the specimen was subjected to a creep stress of 100 Pa. The resulting deformations were measured and recorded. The resiliency of the asphalt binders was evaluated after the first test phase, and then the stress was released and the specimen was

allowed to relax to reach an equilibrium deformation. The elastic recovery can be calculated by a retained deformation that caused the viscous flow to be an irreversible process.

Characterization of Hot Mix Asphalt Concrete (HMAC)

The asphalt concrete briquettes, 4 inches in diameter and 2.5 inches in height, were prepared in the LTRC asphalt laboratory using a standard Marshall Hammer and a Gyratory Testing Machine (GTM). The GTM, Model 8A/6B/4C/1, was manufactured by the Engineering Developments Company, Inc. of Vicksburg, Mississippi. It is a machine that can be used for compaction as well as plane strain and simple shear testing for soils, base course materials, and asphaltic concrete paving mixtures. The GTM produces specimens using a kneading compaction process that is believed to have stress strain properties that are more representative of field compaction conditions.

The engineering properties testing was performed in the LTRC Engineering Materials Characterization and Research Facility (EMCRF) by using the MTS 810 closed-loop controlled servo-hydraulic test system, equipped with an environmental chamber. The machine is rated for 55,000 pounds. Its state-of-the-art digital controller, which is operated under Microsoft Windows NT and MTS Teststar software, conducts the data acquisition and equipment control. The closed-loop consists of a computer and a digital controller acting as the controlling unit over a servovalve, a hydraulic actualic, and test specimen. The initial loading signal is sent from the digital controller to the servovalve, which applies hydraulic pressure on the specimen. The LVDTs, the extensometer, or the force sensor then returns the feedback signal to the controller. The digital controller compares this feedback signal with the control signal and makes adjustments if necessary. The loop is then closed.

Four fundamental tests were conducted to characterize the two mixtures and determine the effects of the CPE binder modification on the properties of HMACs as shown in table 3. The fundamental tests were conducted using a fully automated MTS servo-hydraulic test system. A brief description of each test is given below.

Table 3
Fundamental engineering test methods

Mechanical Test	Property
Indirect Tensile Strength and Strain Test	Tensile strength and strain
Indirect Tensile Resilient Modulus Test	Resilient modulus (stiffness)
Indirect Tensile Creep Test	Creep stiffness modulus
Indirect Tensile Fatigue Test	Fatigue slope and cycles to failure

Indirect Tensile Strength and Strain Test (ITS)

This test was conducted at 25°C according to AASHTO T 245-82. Test specimens were loaded to failure at a deformation rate of 2 inches per minute. The load to failure and horizontal and vertical deformations were monitored and recorded. Figure 2 shows a typical relationship between compressive load and deformation. This test is a relative measure of the tensile properties of the mix that can be related to fatigue endurance characteristics. The indirect tensile strength, S_T, was calculated as follows:

$$S_T = \frac{2P_{ult}}{\pi t D}$$

Where: S_T = indirect tensile strength, psi,
P_{ult} = ultimate applied load to failure, lbf,
t = thickness of specimen, inches, and
D = diameter of specimen, inches.

The indirect tensile strength was reported together with the load to failure and the percent tensile strain, TS, which was calculated as follows:

$$TS = 0.52 * H * 100$$

Where: TS = percent tensile strain,
H = horizontal deformation at failure, inches.

Indirect Tensile Resilient Modulus Test

The testing temperatures used for this test were 5°C, 25°C, and 40°C. The tests were conducted according to the modified ASTM D 4123 *[34]* with the following modifications:

1. Test samples were seated with a sustained load of 20 lbf. A cyclic haversine load of 15 percent, 10 percent, and five percent of the average indirect tensile strength (S_T) at 25°C was then applied to the specimens at 5°C, 25°C, and 40°C, respectively. The two vertical deformations were monitored independently. Further adjustment to the load device was needed if the two measurements exceeded the tolerance level of 10 percent. The average of the two verticals was used in the data analysis as shown in figure 3.
2. With the pre-load applied to the sample, the specimen was conditioned by continuous monitoring of the deformation until the deformation rate was essentially constant. The conditioning was stopped and the transducers were rezeroed.
3. As described in step 1, a haversine waveform load was applied on a repetitive basis with a load frequency of two cycles per second with a 0.1 second loading time and a 0.4 second relation period as shown in figure 4.
4. The instantaneous and total resilient moduli were computed as follows:
   a) The response curves of load, vertical deformation, and horizontal deformation over the two cycles (step 3) were digitized. The data from these curves were then scanned to determine the instantaneous and total recoverable horizontal and vertical deformation. The data at the beginning of the relaxation period were used to compute the instantaneous properties, whereas the data at the end of the relaxation period were used to compute the total properties as follows:

$$M_{RI} = \frac{P(\mu_I + 0.27)}{t\delta H_I} \qquad M_{RT} = \frac{P(\mu_T + 0.27)}{t\delta H_T}$$

$$\mu_T = 3.59\frac{\delta H_T}{\delta V_T} - 0.27 \qquad \mu_I = 3.59\frac{\delta H_I}{\delta V_I} - 0.27$$

Where: M_{RI} = instant resilient modulus, psi,
M_{RT} = total resilient modulus, psi,
μ_I = instantaneous Poisson's ratio,
μ_T = total Poisson's ratio,
P = repeated load, lbf,
t = thickness of specimen, inches,
ΔH_I = instantaneous recoverable horizontal deformation, inches,

ΔH_T = total recoverable horizontal deformation, inches,

ΔV_I = instantaneous recoverable vertical deformation, inches,

ΔV_T = total recoverable vertical deformation, inches.

b) Both the average resilient modulus, M_R, and the average Poisson's ratio (for both instantaneous and total) were calculated as:

$$M_R = \frac{\sum_{i=1}^{4} M_{R(i)}}{4} \qquad \mu = \frac{\sum_{i=1}^{4} \mu_{(i)}}{4}$$

Following steps 1 through 4, each specimen was tested at each of the three temperatures, starting with the lowest temperature, to minimize permanent damage to the sample. The individual specimen was tested in its initial position, and the sample was then rotated approximately 45 degrees to repeat steps 1 through 4.

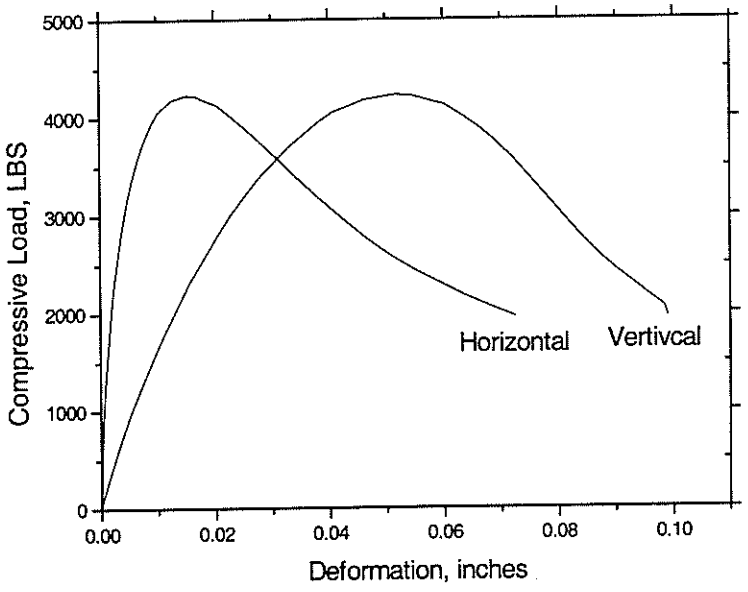

Figure 2
Typical compressive load vs. deformation for the indirect tensile strength and strain test *[35]*

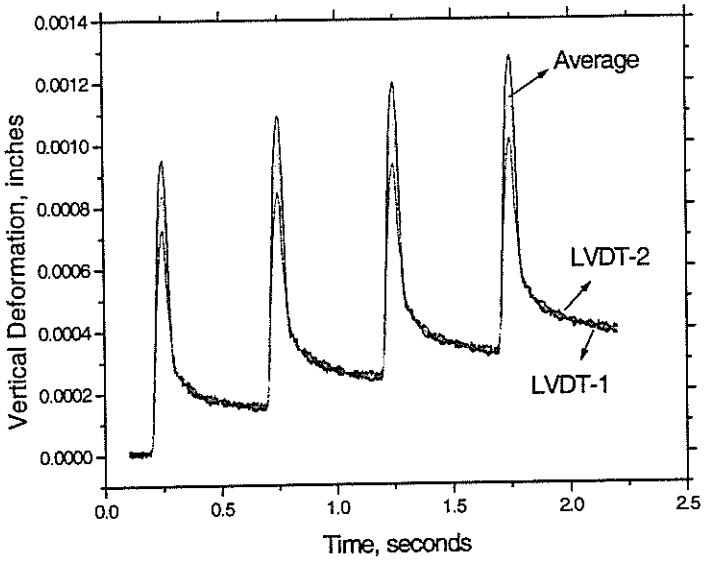

Figure 3
Typical vertical deformation vs. time diagram for the indirect tensile resilient modulus test

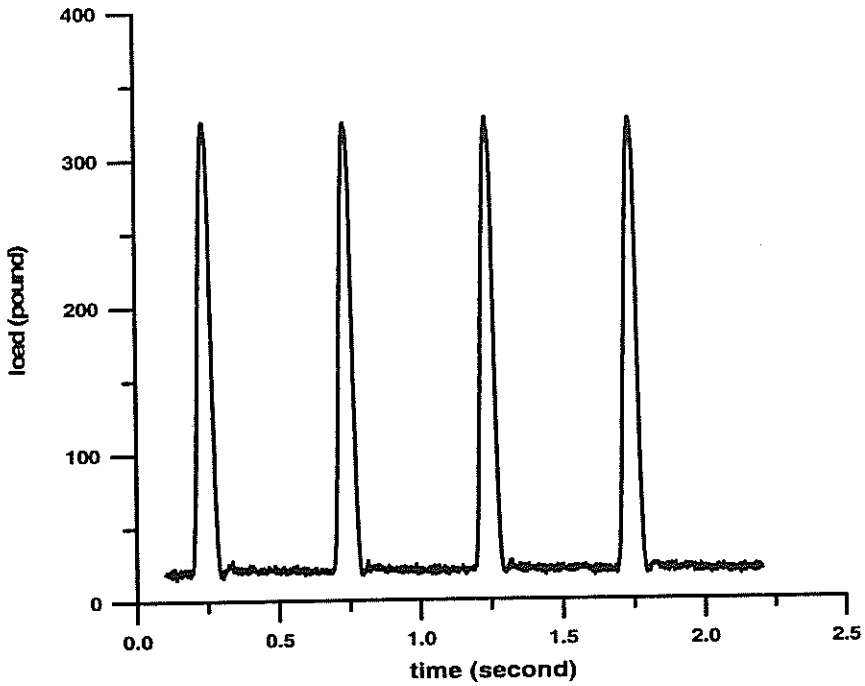

Figure 4
Typical load vs. time diagram for the indirect tensile resilient modulus test

Indirect Tensile Creep Test

To evaluate the rutting potential of asphaltic concrete mixtures, this test was conducted by using the creep slope and the time to failure characteristics. The creep test was conducted using a ramp load of 250 pounds at 40°C applied as quickly as possible, using the stress-control mode of the MTS servo-hydraulic system. The load, vertical, and horizontal deformation were recorded continuously with the data acquisition system.

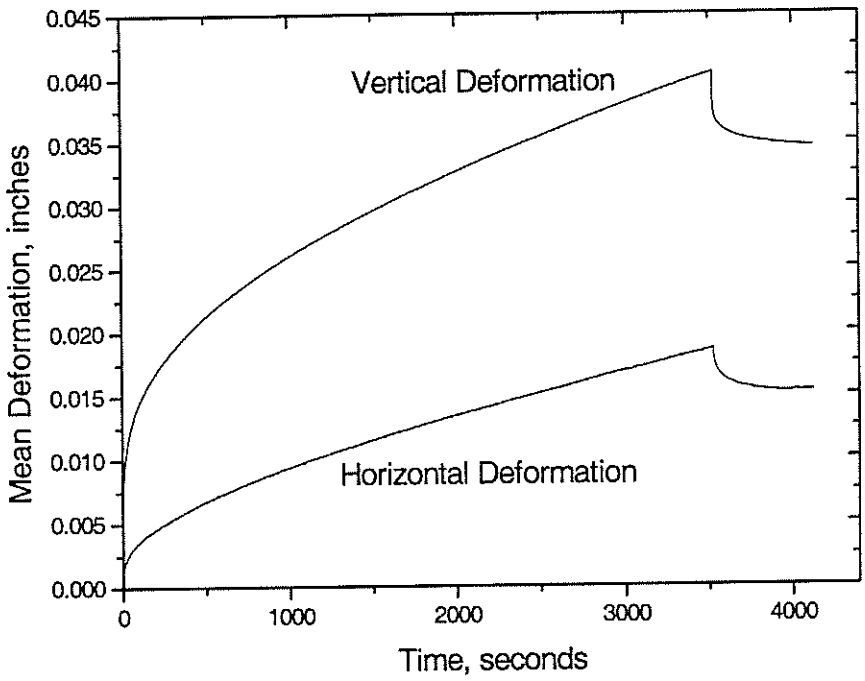

Figure 5
Typical creep deformation vs. time relation

The test was terminated either after 60 minutes of load duration or until sample failure. Figure 5 presents a typical creep deformation-time relationship. The creep modulus C(t) was computed as follows:

$$C(t) = \frac{(-3.59) * P_0}{T * \Delta V(t)}$$

Where: C(t) = creep modulus (stiffness) at time t, psi,
P_0 = applied vertical load, lbf,
μ = Poisson's ratio,

T = specimen thickness, inches,

ΔV (t) = vertical deformation at time t, inches.

In order to obtain the creep modulus, C(t), the log of the creep modulus was plotted against the log of the time to sample failure as represented in figure 6. From this plot the creep slope of the calculated indirect tensile creep modulus and the time to failure were obtained and later used in the statistical analysis.

Indirect Tensile Fatigue Test

To determine the fatigue resistance of the asphalt concrete samples, this test was conducted at 25°C. A haversine type cyclic load with a peak value corresponding to 10 percent of the ITS was applied. This load was applied on a repetitive basis with a load frequency of two cycles per second with a 0.1 second loading time and a 0.4 second relaxation period. The horizontal deformations were monitored through the duration of the test, and the test was terminated when the total horizontal deformation reached 0.1 inch *[36]*. In order to obtain the fatigue slope and the number of cycles to failure, the log of the permanent horizontal deformation was plotted against the log of the number of cycles to sample failure as shown in figure 7.

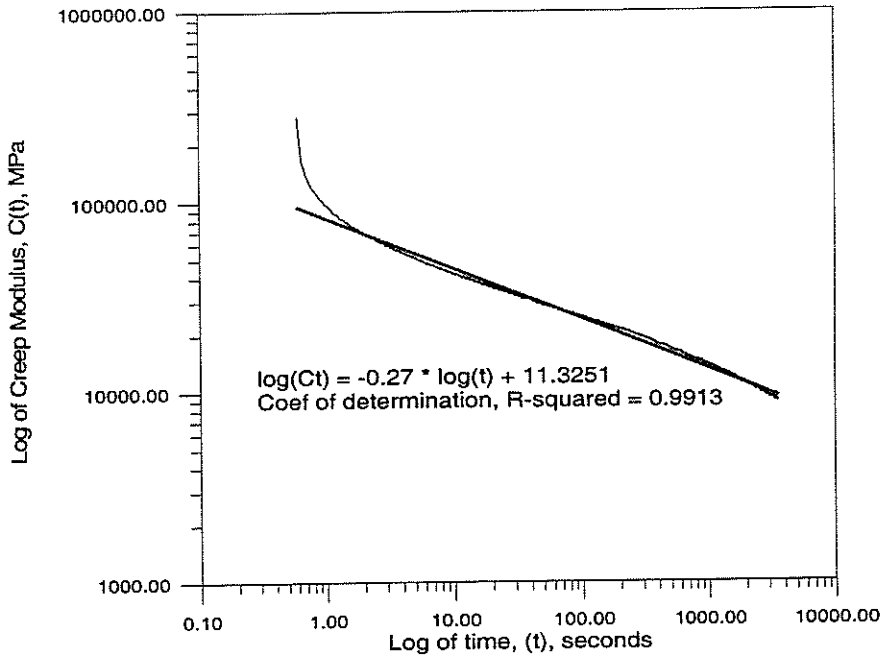

Figure 6
Typical plot of indirect tensile creep data

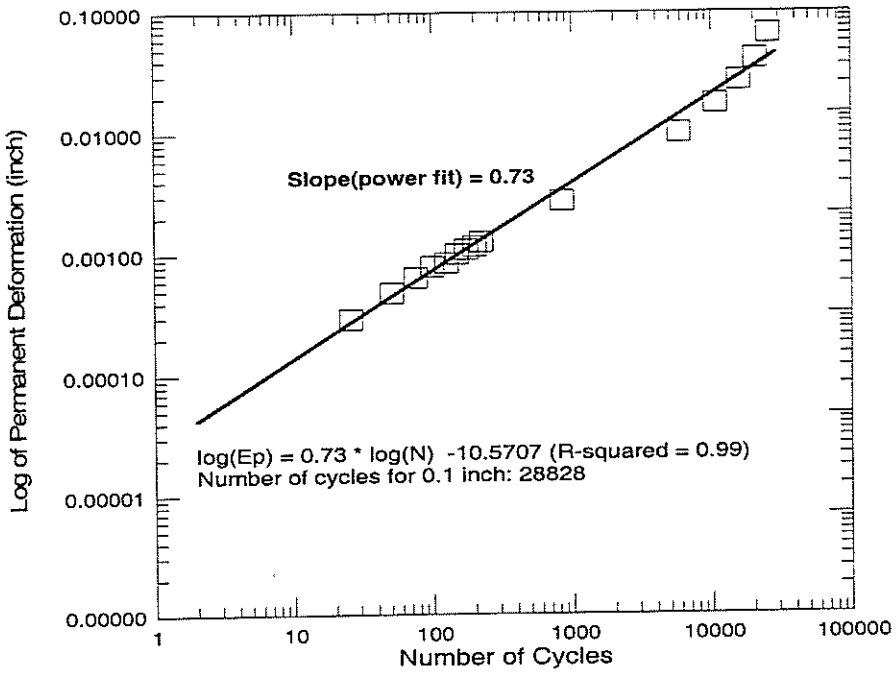

Figure 7
Plot of permanent horizontal deformation vs. number of cycles to sample failure

Data Analysis

The results of these tests were statistically analyzed using the analysis of variance (ANOVA) procedure provided in the Statistical Analysis System (SAS) program from SAS Institute, Inc. A multiple comparison procedure with a risk level of five percent was performed on the means. The tables for the grouping present the mean for the test results reported by mixture type. The group rows contain the results of the statistical grouping reported with the letters *A, B, C,* and *D*. The letter *A* was assigned to the highest mean followed by the other letters in appropriate order.

DISCUSSION OF RESULTS

Preparation and Characterization of Polymers

Polyolefins, in particular high density polyethylenes, are highly crystalline. The crystalline regions of the polymer are very useful as reinforcing structures, but they exhibit very little compatibility with asphalts. Chlorination of PE disrupts the crystalline regions and introduces some polar components with higher asphalt compatibility along the chain. The physical properties of CPE are dependent on chlorine content and chlorine distribution, which in turn are determined by the technique used for chlorination. Chlorination can be carried out in a homogeneous phase (solution method) or in a heterogeneous phase (suspension method). The microstructure and morphology of CPE's have been reported *[37], [38]*, and the factors controlling these parameters are documented.

In solution chlorination, chlorine atoms attack the polymer in a random manner; the resultant homogeneous distribution of attached chlorine atoms destroys the ordered arrangement of the PE chain so that the crystallinity of the polymer decreases (scheme 1). In this work, it limits the discussion to CPE's prepared in solution. Preparations of CPE's for this study in various contents were carried out at 115°C in 1,1,2,2-tetrachloroethane (TCE). The results of the polymer modification are summarized in table 4.

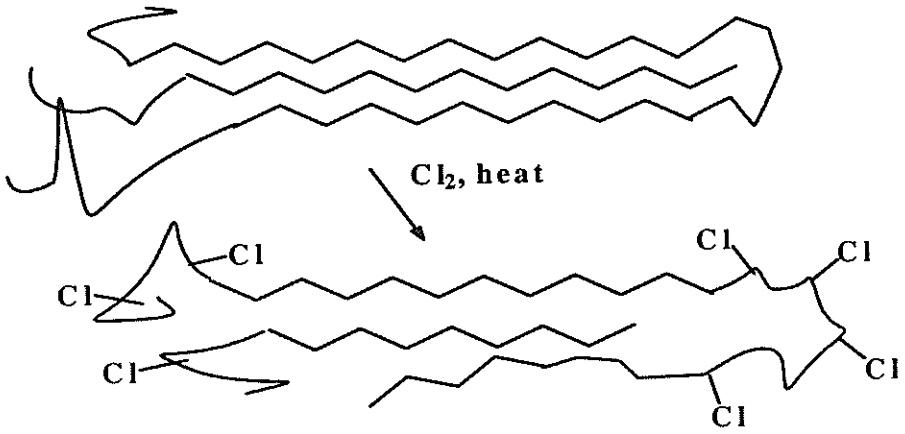

Scheme 1
Chlorination of Polyethylene

The chlorine content and chlorine distribution were analyzed with proton NMR. The melting point and crystallinity were determined by DSC data. The ^{1}HNMR spectra of HDPE and CPE are shown in figure 8. The HDPE spectrum is primarily one single peak corresponding to -CH_2- unit. However, a chlorinated polyethylene spectrum, which was prepared in a solution chlorination, exhibits two main peaks corresponding to -CHCl-, 3.8~4.7 ppm, and -CH_2-, 1.0~2.7 ppm. In solution chlorination, the randomly attached chlorine atom destroys the ordered arrangement of the polyethylene chain. When comparing the methylene signal of HDPE with CPE, more peaks are shown in the range from 1.5~2.5 ppm because the -CH_2- units next to the -CHCl- units are different. For instance, if there is a randomly distributed chlorine along the polymer chain, such as the -CHCl-C*H_2-CHCl-C**H_2-C***H_2-C**H_2 -CHCl- structure of CPE, then there will be at least three assignments of chemical shifts of methylene units (designated by *, **, and ***, in a NMR spectrum). The hydrogen attached to a chlorine-containing carbon appears as a signal downfield, in range from 3.8~4.7 ppm. Based upon the relative areas of these peaks, the chlorine contents of the two CPE's used in this study are CPEA, 5.8 weight percent, and CPEB, 24.5 weight percent. The DSC thermograms of chlorinated HDPEs showed significant changes in the melting points and heats of fusion (ΔH_f) relative to those observed with the starting HDPE. Both the shift in the melting transition and the reduction in the ΔH_f are consistent with the reduction in crystallinity induced by the chlorination.

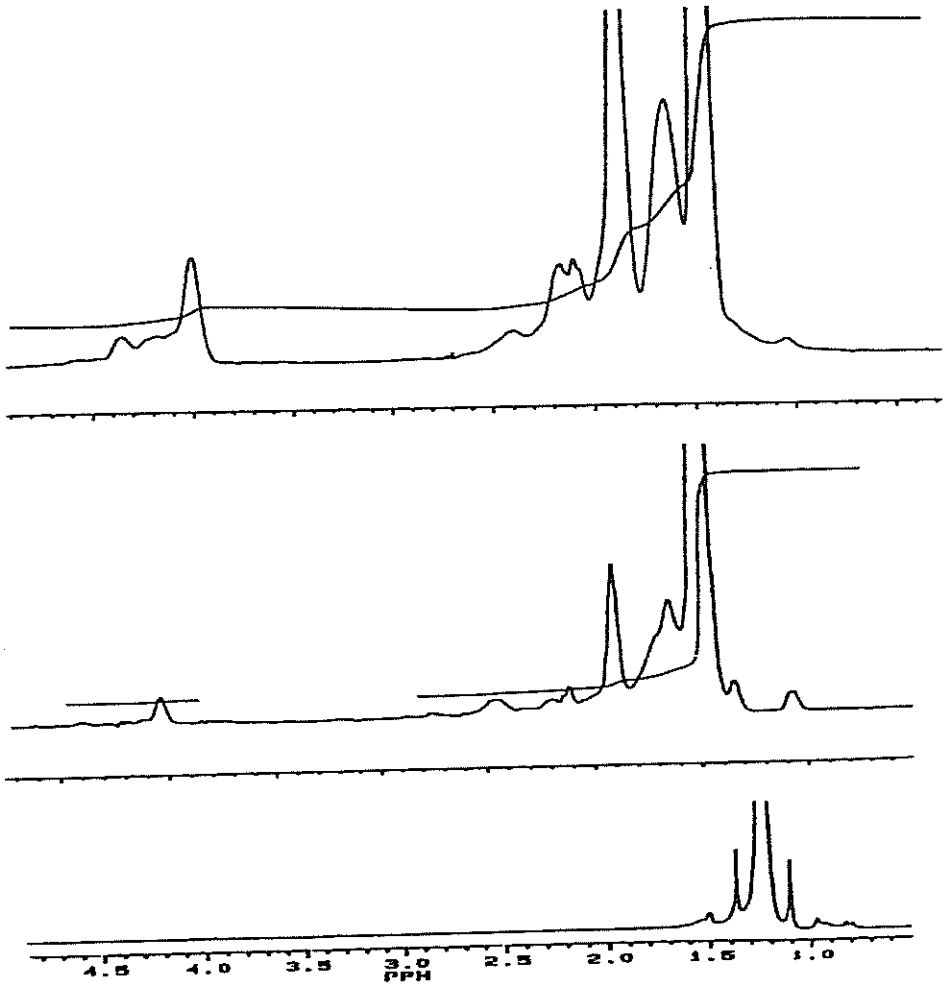

Figure 8
^{1}HNMR spectra of HDPE (bottom) and chlorinated polyethylenes, CPEA (middle) and CPEB (top)

Table 4
NMR and DSC characterization of HDPE and chlorinated HDPE

Polymer	% Chlorination	Melting Temperature	ΔH_f	Crystallinity*
HDPE	0	131°C	202.2	74.9%
CPEA	5.8	119°C	145.8	54%
CPEB	24.5	45-70°C	34.8	12.9%

* The percent crystallinity was estimated from this data by assuming that 100 percent completely crystallized hydrocarbons exhibit an average enthalpy of 270 Joules/gram (J/g) *[39]*.

Modification of Polypropylene

Maleic anhydride modified polymers are specialized materials because the pendent anhydride moiety provides functionality for cross-linking and other chemical modifications. The free radical promoted addition of MAH to polyolefins is a well documented technique *[40], [41], [42], [43]* due to its simplicity and effectiveness (scheme 2). In fact, a commercial extrusion process for reacting MAH with PP is currently being run at the Adell Plastics plant in Denham Springs, LA. It is necessary to explore the potential applications of this maleated polypropylene as an asphalt modifier.

First, it was important to determine the extent of maleation achieved in the Adell process. A comparison of FTIR spectra (figure 9) of SAH, MAH, MPP, and PP shows that MPP, SAH, and MAH have bands characteristic of cyclic anhydride at 1781 cm^{-1} and 1720 cm^{-1}. No bands appear in this region of the PP spectrum. Also in the MPP spectrum, the intensity of the few characteristic bands of PP diminishes. This indicates that the carbonyl peak of MPP apparently results from the grafting of SAH groups onto the polypropylene backbone. Based upon the calibration curve for SAH in PP vs. carbonyl index (figure 1), the degree of maleation of the commercial product in MPP was found to be 1.28 weight percent. The low concentration did not make a significant impact on the degree of crystallinity of PP (table 5), but it did enhance its compatibly with asphalt.

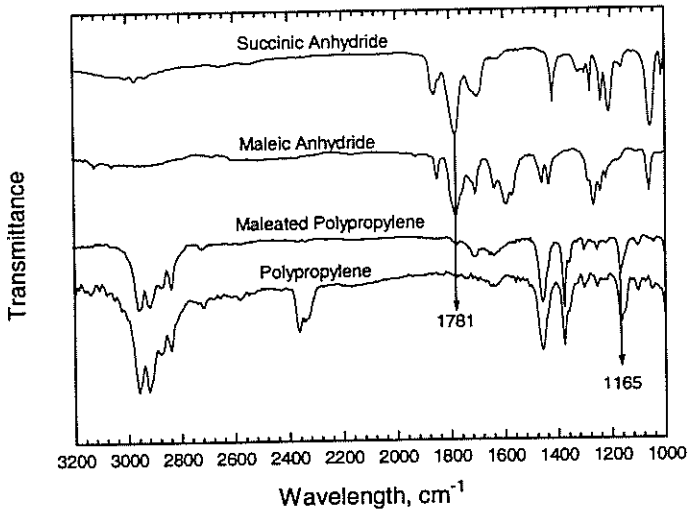

Figure 9
FTIR Spectra of succinic anhydride (SAH), maleic anhydride (MAH), maleated polypropylene (MPP), and polypropylene (PP)

Maleated polypropylene (MPP) was blended with selected asphalts, and a high degree of compatibility was noted. One concern would be that the high reactivity of the anhydride functional group could cause the blends to change character on storing, but no significant changes in the viscosity of the blends were detected after they had been heated at 135°C for 24 hours. One can reduce the potential reactivity of the maleated polymer by allowing it to react with several different monofunctional amines to produce maleimide derivatives with different degrees of polarity (scheme 2). These reactions were conducted in the melt to simulate reactions that could be conducted in an extruder. Also a blend of PVA and MPP can be prepared in the melt in an effort to substantially enhance the hydrophilic character of the polymer additive. The composition and properties of the maleated polypropylene derivatives are summarized in table 5.

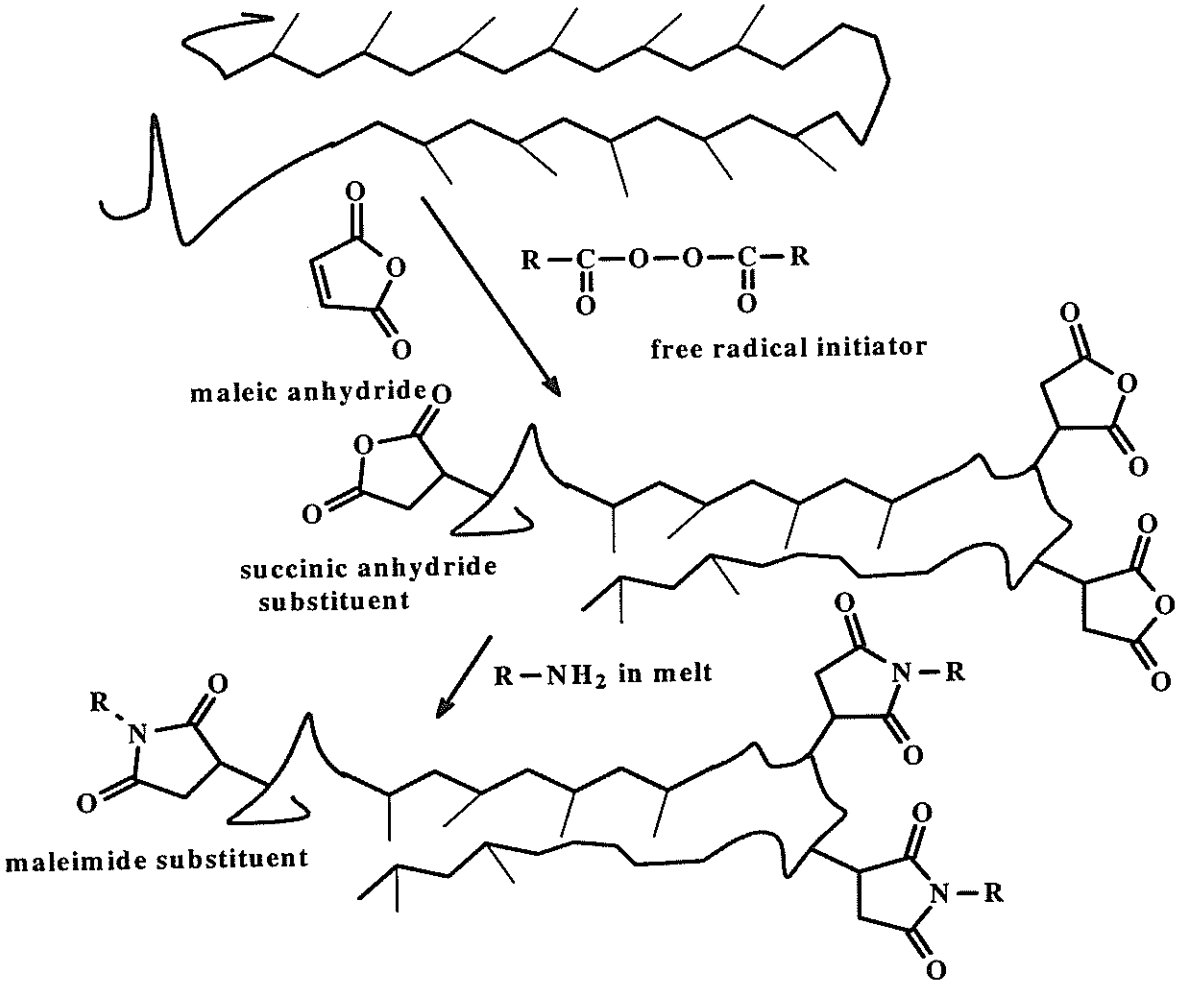

Scheme 2
Modification of polypropylene by maleation and subsequent polyimide formation

Table 5
Composition and properties of maleated polypropylene derivatives

Polymer	% Subst.	Tm, °C	ΔH_f, J/g	% Crystallinity
Polypropylene,PP	0	166.3	94.4	45.2
MPP (Adell)	1.28	166.7	91.4	43.7
Polyvinyl alcohol adduct, MPPPVA	1.39	163.9	88.9	42.5
Ethanolamine adduct, MPPEA	1.25	164.6	121.9	58.3
Ethanolamine adduct, prepared in Haake, MPPEAH	2.47	166.7	92.4	44.2
Naphthyl amine adduct, MPPNA	1.23	167.1	113.0	54.1
N-aminomorpholine adduct, MPPAM	1.25	165.9	106.8	51.1

The percent crystallinity of the modified samples was based upon the reported theoretical ΔH_f of PP of 209 J/g *[43]*. None of the modifications reduced this crystallinity to a significant extent. In fact, the crystallinity of the polyimide derivatives increased slightly. However, all the polymers contained a minimum of 45 percent amorphous region, where the interaction with the non-polar asphalt components is focused. The main contribution of maleation and subsequent modification was to improve interactions with the polar asphalt components.

Thermal Properties of Asphalt

The thermal behavior of asphalts is complex and depends on their sources, methods by which they are manufactured, and thermal history. The thermal history of an asphalt sample exerts a critical influence on the relative crystallinity of the asphalt/polymer components and on the corresponding DSC thermographs obtained from the samples *[5]*. The transition of amorphous liquids to crystalline regions in polymeric substances is controlled by kinetic factors *[44]*. Although asphalts are not high molecular weight polymers (average molecular weight of 700 -1000), they can have quite high viscosities around room temperature. When the kinetic complications imposed on the formation of crystals in asphalts are combined with component complexity, the rate of crystalline region formation in a given asphalt can be very slow. Slow heating or annealing before analysis is required to approach equilibrium and eliminate the effects of previous thermal histories.

Figure 10 is an example of a DSC thermogram of a typical Louisiana ACL-1 asphalt showing only two transition temperatures (Tr) at 13°C and 53°C. To reveal the complexity of a given asphalt binder, it is necessary to anneal the sample at temperatures slightly below the expected transitions. Therefore, a staged annealing program *[5], [45]* was developed when the sample was initially heated to 100°C. It was then cooled at 10°C per minute from 100°C to 20°C and held 24 hours at 7°C (refrigerator) and -5°C (freezer), consecutively (figure 11).

Using these conditions, DSC measurements were conducted on two SHRP core asphalt samples that were selected by a special panel to represent asphalts from different sources. These samples were analyzed in several laboratories *[7], [8], [9]* without applying an annealing process. The authors implied that most asphalts contain very similar crystallizable components.

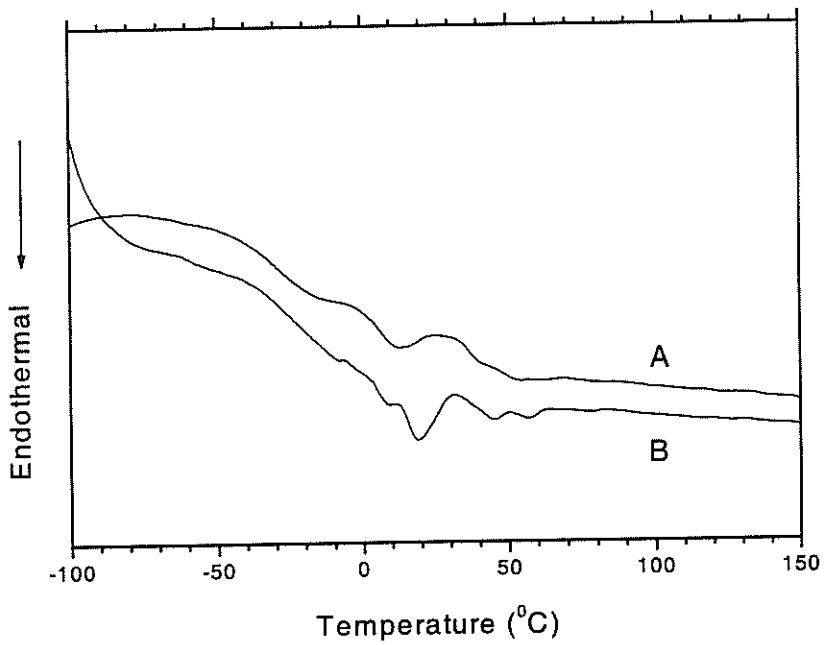

Figure 10
DSC thermograms of asphalt ACL-1 measured 10°C /min under nitrogen: A, no annealing, first heating; B, after staged annealing illustrated in figure 11

The identical endothermic patterns they observed were taken as thermal responses from identical molecular structures. However, this hypothesis conflicts with the observed complexity in asphalt molecular structures *[3], [46]*. Using the annealing sequences, the

thermal transitions exhibited by individual asphalts can be resolved. As shown in figure 12, standard asphalt ABC-1 exhibited only two broad endothermic transitions at 24.0 and 42.6°C.

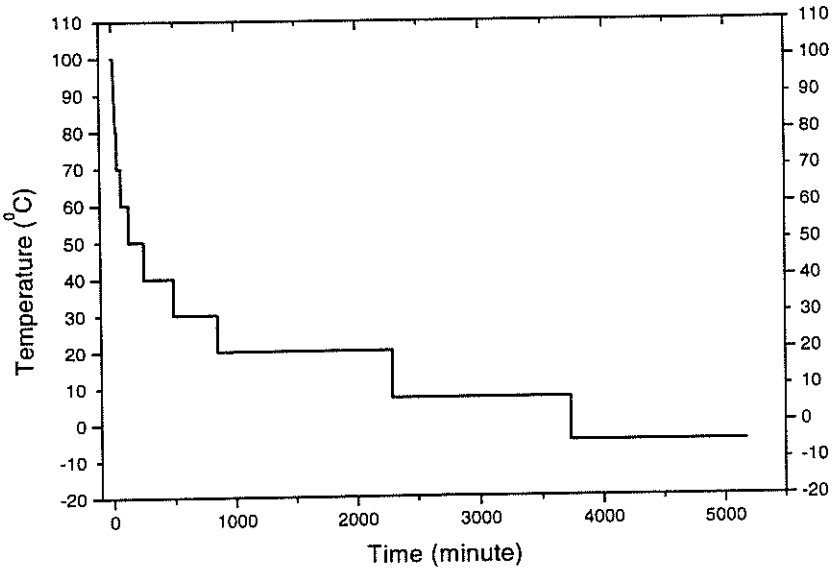

Figure 11
Staged annealing program for asphalt samples. Stages as follows: 100°C, 10 min.; 80°C, 30 min.; 70°C, 30 min.; 60°C, 60 min.; 50°C, 120 min.; 40°C, 240 min.; 30°C, 360 min.; 20°C, 1440 min.; 7°C, 1440 min.; -5°C, 1440 min.

After subjecting the sample to annealing, five transitions could be identified at the following temperatures: -27.0°C, 1.9°C, 14.1°C, 38.4°C, and 52°C. In contrast, the main features in the thermogram of standard asphalt AAD-1 (figure 13) consisted of two endothermic transitions at 16.6°C and 42.7°C. Annealing this sample did not produce a significant change in the thermogram. Clearly, the composition of sample ABC-1 is much richer in crystallizable components, but studying annealed samples can only identify this distinction.

Identification of Asphalt Sources

The influence of component complexity on the crystallization process was demonstrated by examining a series of asphalts. The annealing program, shown in figure 11, was applied to the five Louisiana asphalt samples described in table 6. The corresponding thermograms are shown in figure 14 A-E, respectively. After annealing, it is clear that not all thermograms of the five asphalt samples exhibit the same pattern of endothermic transitions. Careful inspection of the thermograms in figure 14 reveals that there are distinct patterns for each sample. Thus, the annealing technique combined with DSC measurements may provide a

simple method to identify the source of an unknown asphalt, providing that thermograms are available for asphalts from a wide variety of sources.

Table 6
DSC characterization of Louisiana asphalt samples

Sample	ACL-1	ACL-2	ACE-1	ACM-3	ACR-3
Source	Lion	Lion	Eagle	Marathon	Ergon
Grade	AC-10	AC-20	AC-10	AC-30	AC-30
Number of Endothermic Transitions	5	5	4	3	1
ΔH_f (J/g)[a]	2.63	5.1	6.1	4.28	0.3
% Crystallinity[b]	1.31	2.55	3.05	2.14	0.15

[a] Determined on annealed samples measured at 5°C/min.
[b] Average entropy for 100 percent crystallinity = 200 J/g *[8]*

Compatibility Analysis by Differential Scanning Calorimetry

The application of DSC analysis of asphalts and asphalt polymer blends to evaluate interaction of the asphalt components have been reported *[47]*. A comparison of DSC thermograms of HDPE, tank ACL-1, and ACL-1/3 percent HDPE showed no significant changes in the asphalt transitions between the tank asphalt and the asphalt/polymer blend (figure 15). The HDPE (curve A) has a melting peak at 130.7°C, while the heat of fusion (ΔH_f) is 202 J/g.

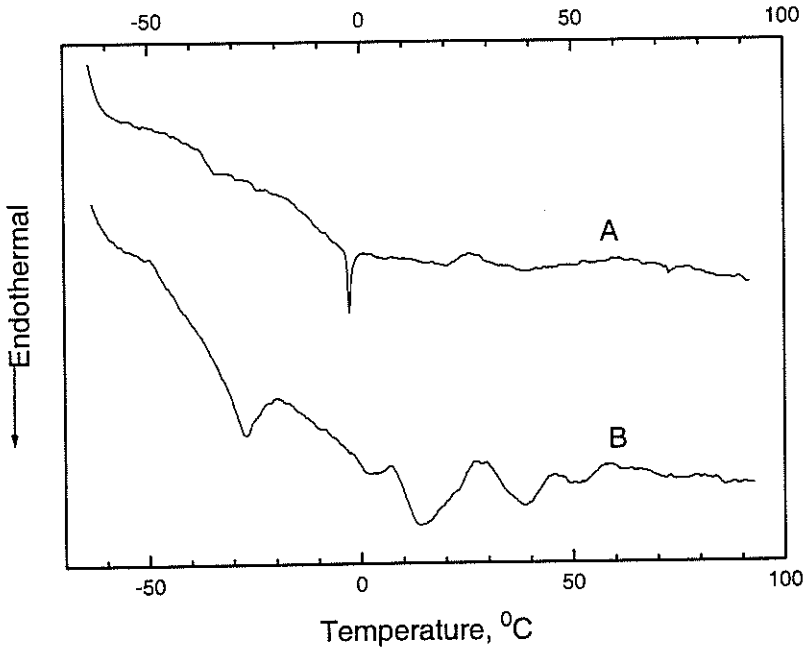

Figure 12
DSC thermograms of standard asphalts before and after the samples were subjected to the annealing: A, ABC-1; B, annealed ABC-1

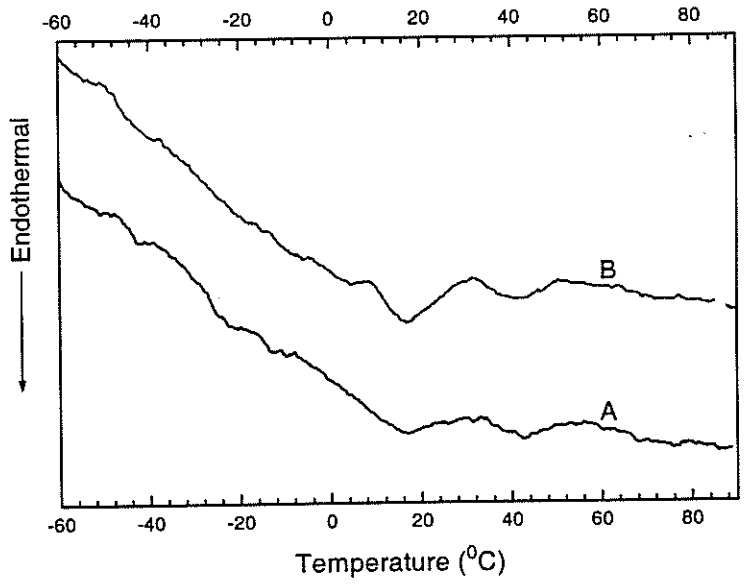

Figure 13
DSC thermograms of standard asphalts before and after the samples were subjected to annealing: A, AAD-1; B, annealed AAD-1

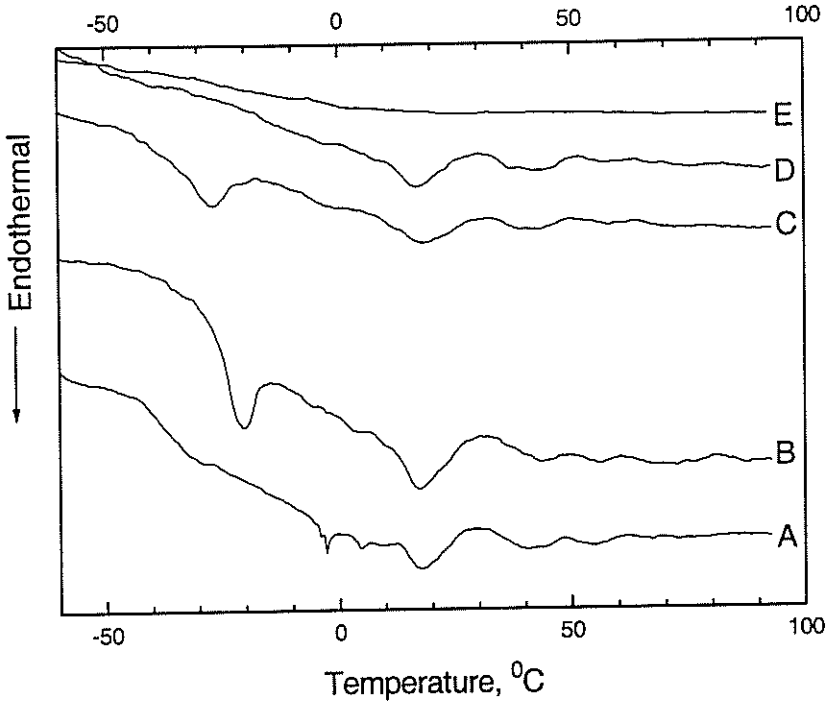

Figure 14
DSC thermograms of annealed Louisiana asphalt samples: A, ACL-1; B, ACL-2; C, ACE-1; D, ACM-3; E, ACR-3

However, in the AC-10/3 percent HDPE blend (curve C), the melting point shifts down to 120°C, and the heat of fusion (ΔH_f = 6.0 J/g) is approximately three percent of that observed for HDPE. This phenomenon indicates that most HDPE crystallinity remains intact in the blend. The DSC thermograms of CPEA (5.8 weight percent Cl), annealed tank ACL-1, annealed ACL-1/3 percent CPEA, and annealed ACM-1/3 percent CPEA are shown in figure 16. The melting transition of pure CPEA is 119°C and the ΔH_f = 146 J/g (curve A). When this polymer was blended with asphalt, the annealed ACL-1/3 percent CPEA blend (curve B), the melting transition shifted to 113°C and the ΔH_f for this transition was 2.8 J/g. If the crystallinity of the CPEA were retained, a value for the ΔH_f of 4.38 J/g would be expected. The discrepancy between the observed and calculated ΔH_f suggests that there is an interaction between CPEA and asphalt that affects crystallization of both materials. Note that the interaction of ACM-3 with CPEA is slightly less than that observed for the ACL-1 samples. The asphalts from different sources tend to yield blends with slightly different properties.

Another comparison of DSC thermograms of ACL-1 blended with 3 percent HDPE or chlorinated HDPE is shown in figure 17. One can observe that endothermic transition of curve A is shifted down to 113°C (curve B) and 46°C (curve C) as the chlorine contents increase in HDPE, i.e., to the temperature range where the crystalline fractions of the asphalt cement melt.

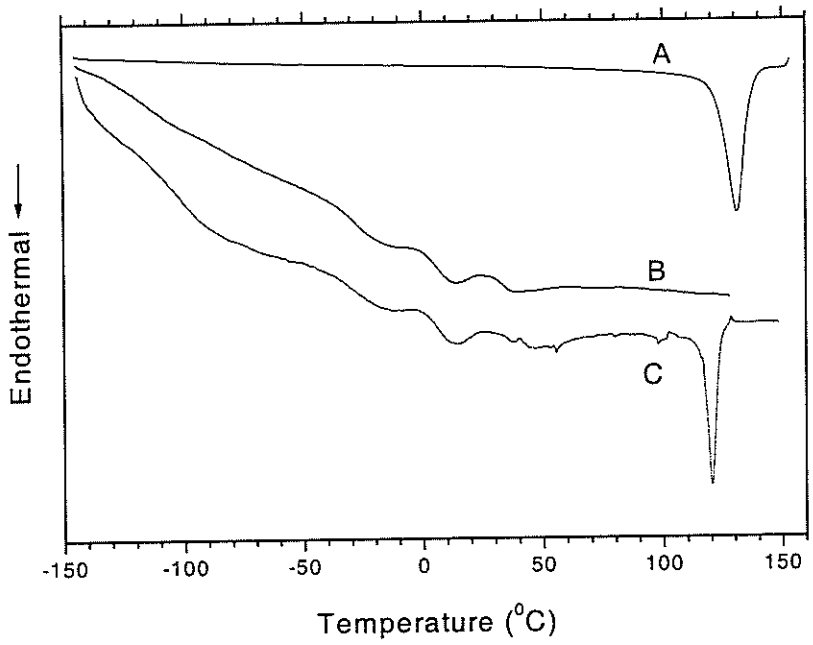

Figure 15
DSC thermograms of: A, HDPE; B, asphalt ACL-1; and C, asphalt ACL-1/3 percent HDPE blend

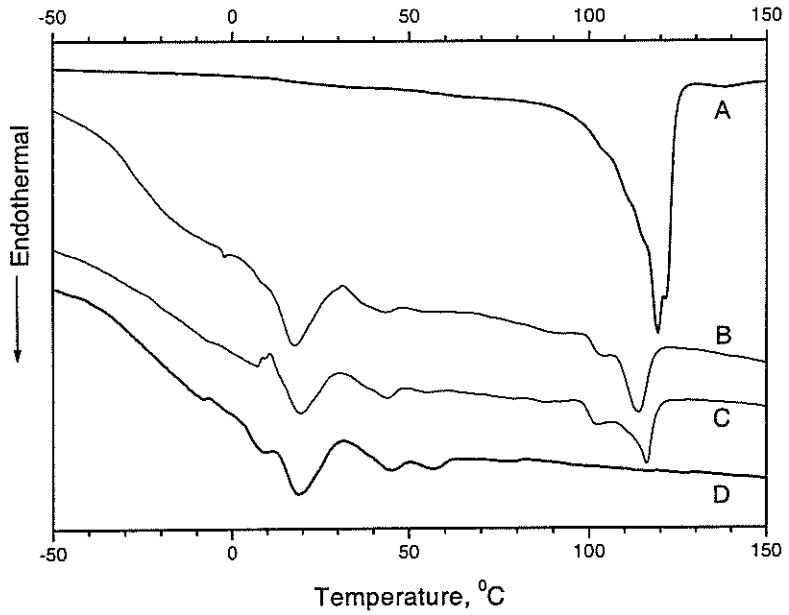

Figure 16
DSC thermogram of: A, CPEA; B, annealed ACL-1/3 percent CPEA; C, annealed ACM-3/3 percent CPEA; and D, annealed ACL-1

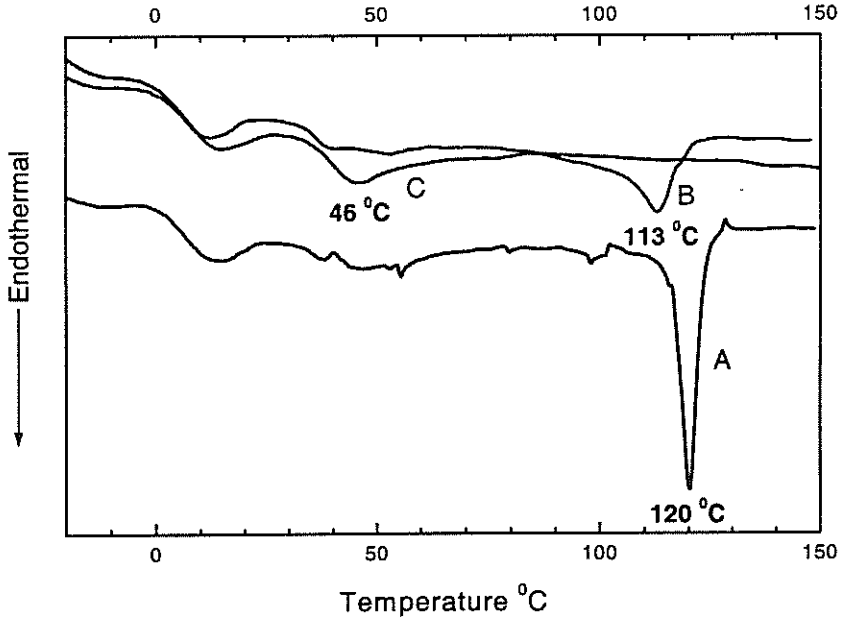

Figure 17
DSC thermograms of: A, ACL-1/3 percent HDPE; B, ACL-1/3 percent CPEA; C, ACL-1/3 percent CPEB

The introduction of chlorine atoms to the HDPE backbone changes the polarity and reduces the crystallinity of the polymer (CPEA or CPEB). The modification of the polymer adjusts the interaction parameters by both increasing the amorphous content and enhancing the interaction of the amorphous regions of the polymer with the asphalt phase.

Enhanced interaction of polyolefins with asphalt can also be achieved by maleation. The introduction of approximately 1.3 weight percent SAH units by treatment of PP with MAH in the presence of a free radical initiator enhances the polarity of the polyolefin. The DSC thermograms, shown in figure 18, for blends of MPP with ACR-3 show a clear reduction in the maleated polypropylene melting transition at 165°C to a broader, less intense transition around 155°C. Further modifying the SAH substituents with amines did not change the interaction significantly.

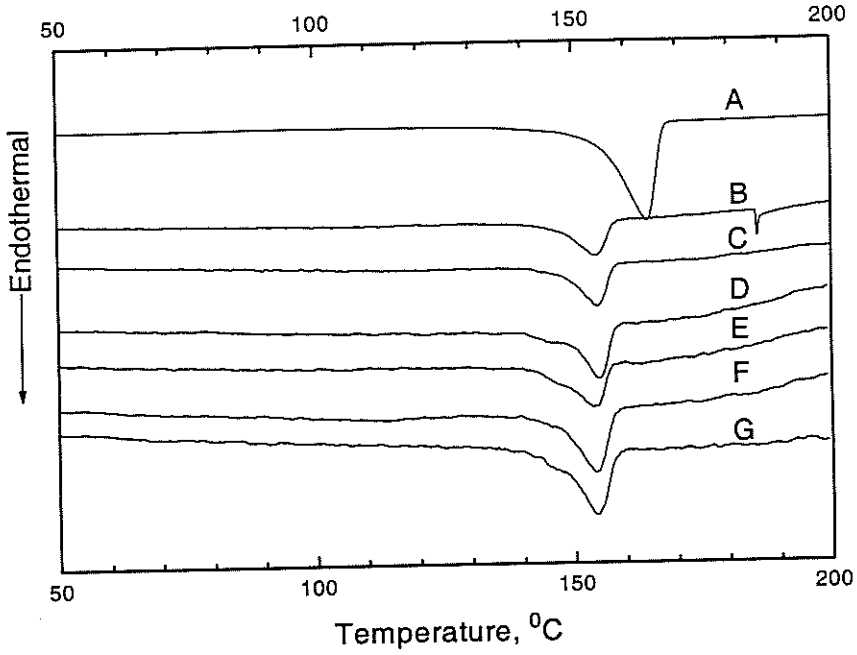

Figure 18
DSC thermograms of: A, MPP; B, ACR-3/3 percent MPPAM; C, ACR-3/3 percent MPPEAH; D, ACR-3/3 percent MPPEA; E, ACR-3/3 percent MPPPVA; F, ACR-3/3 percent MPP; G, ACR-3/3 percent MPPNA

Combining the MPP with PVA also failed to change the thermogram of the blend. Simply introducing the succinic anhydride substituents was sufficient enough to improve the compatibly of polypropylene with asphalt.

Microscopic Behavior of Asphalt/Polymer Blends

Asphalt/polymer structures were viewed with ESEM to examine asphalt/polymer phase distribution and structural changes at different temperatures. Figure 19 shows the ESEM image of tank asphalt, ACL-1, without any modifier after it was heated to 120°C and cooled down to 40°C. After a similar thermal treatment, an ESEM micrograph of an ACL-1 blend with three percent HDPE cooled from 130°C to 35°C shows particles of HDPE clearly separated from the asphalt (figure 20). The specimen, in which an asphalt ACL-1 was blended with three percent CPEA (5.8 weight percent Cl) and cooled from 130°C to 35°C, shows that partial phase separation also exists in the asphalt/chlorinated polyolefin blend (figure 21). After raising the temperature to 64°C, the melting of the asphalt/polymer blend was clearly observed (figure 22).

Comparing figure 20 (asphalt/HDPE) and figure 21 (asphalt/CPE) confirms that the CPE rich phase was larger than the corresponding HDPE rich phase in the asphalt blends. More highly dispersed polymer rich phases are expected to improve the toughness of brittle asphalt at low temperatures and reinforce asphalt at high temperatures *[48]*. Another image of an asphalt blend with three percent CPEB (24.5 weight percent Cl) examined at 35°C after heating to 130°C is shown in figure 23. There is no clear-cut boundary between the asphalt and synthetic polymer in the asphalt/CPEB (24.5 weight percent Cl) blend whereas the other asphalt/CPEA (5.8 weight percent Cl) blend shows a boundary between asphalt and polymer. The contrast between the two asphalt blends shows that the chlorine content in HDPE is a significant factor in controlling its compatibility with asphalt.

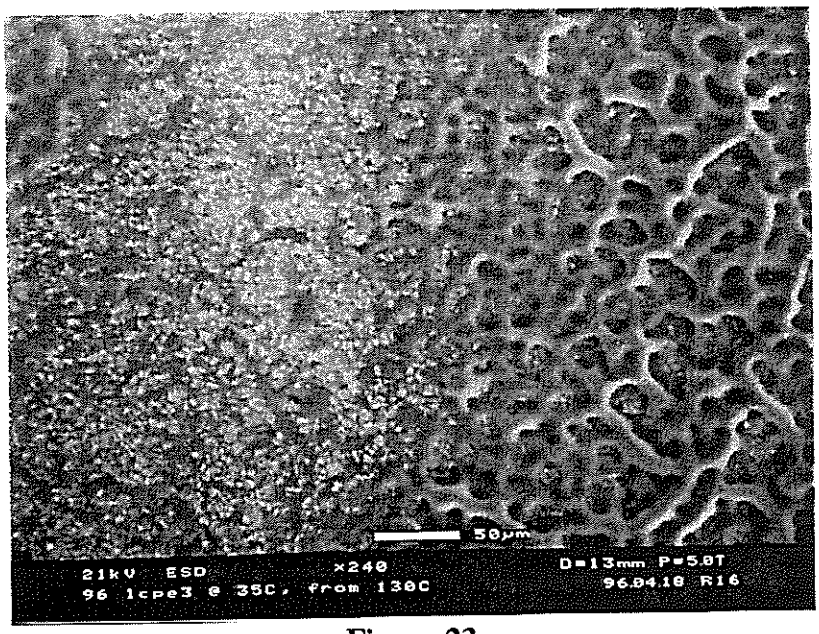

Figure 23
ESEM of Tank ACL-1/3 percent CPEB (24 weight percent Cl) heated to 130°C then cooled to 35°C; magnification x 240

Viscosity of Asphalt and Polymer Modified Asphalt Blends at High Temperatures

A Brookfield viscometer was used to evaluate the handling and pumping properties of asphalt binders at high temperatures. A Superpave PG specification suggests that the viscosity of asphalt binders at 135°C should be less than three Pa·s in order to ensure that the binders can be adequately pumped and mixed with the aggregates. The impact of each aging step, TFOT and PAV, was measured at 135°C. The data in figure 24 show that the viscosity increases upon aging for both tank and polymer modified asphalts, but ACL-1 blends containing three percent HDPE or CPE could be produced and stored without their viscosities exceeding the three Pa·s specification. As will be confirmed by DSR measurements, asphalt blends containing CPE exhibited higher viscosity initially and after PAV aging due to better compatibility between this polymer and the polar components from the asphalt.

A compilation of the viscosity data for each of the blends prepared for this project is found in table 7. Note that in no case does the viscosity of a blend exceed the proscribed three Pa·s upper limit. Furthermore, it appears that the presence of compatible polymer additives does not impact aging. In most cases the PAV/original viscosity ratios of the blends were comparable to those observed for the tank asphalts.

Table 7

Influence of asphalt type and polymer type on viscosity,η, Pa·s @ 135°C, 100 rpm, of original, TFOT, and PAV asphalt binders

Sample	% Add	Original	TFOT	PAV	PAV/Original
ACL-1	0	0.243	0.440	0.518	2.13
ACL-1/HDPE	3	0.635	0.985	1.267	2.00
ACL-1/CPEA	3	0.828	0.935	1.470	1.78
ACL-1/CPEB	3	0.620	1.097	1.550	2.50
ACE-1	0	0.155	0.575	0.820	5.29
ACE-1/HDPE	3	0.190	1.217	1.685	8.87
ACE-1/CPEA	3	0.265	1.247	2.210	8.34
ACE-3	0	< 0.05	0.495	1.127	-
ACE-3/SBS (PAC40)	3	**1.125**	**1.300**	**≥ 2.50**	**≥ 2.22**
ACM-3	0	0.475	0.775	1.140	2.40
ACM-3/HDPE	3	0.725	1.110	1.935	2.67
ACM-3/CPEA	3	0.965	1.535	2.250	2.33
ACR-3	0	0.425	0.400	0.693	1.63
ACR-3/HDPE	3	0.850	1.152	1.860	2.19
ACR-3/CPEA	3	0.760	1.332	2.410	3.17
ACR-3/MPP	3	0.855	1.007	1.307	1.53
ACR-3/MPPPVA	3	0.900	0.780	1.375	1.53
ACR-3/MPPEAH	3	0.828	0.785	1.295	1.56
ACR-3/MPPNA	3	0.875	0.940	1.322	1.51
ACR-3/MPPAM	3	0.840	1.020	1.540	1.83
AAD-1	0	0.170	0.678	1.465	8.62
ABC-1	0	0.340	0.850	1.450	4.27

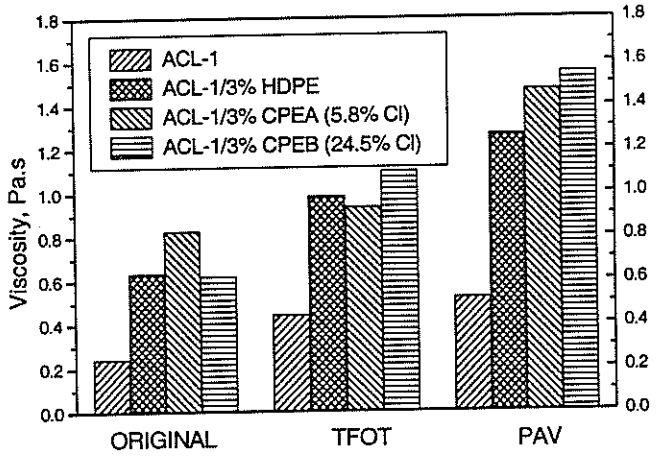

Figure 24

Influence of an ACL-1 and polymer types on viscosity of original, TFOT, and PAV binders at 135°C

Blend Rheology

Dynamic shear tests are advantageous because the data can be acquired within the linear range of the asphalt in a loading mode that is similar to traffic loading. These measurements are particularly useful in the transition region, where delayed elasticity is a major portion of the material response. A dynamic shear rheometer was used to measure the linear viscoelastic moduli of asphalt cement binders under oscillating conditions to yield dynamic mechanical properties. G*, the ratio of the peak stress to the peak strain, reflects the total stiffness. The in-phase component of IG*I is the shear storage modulus, G' (the elastic portion), the out-phase component of IG*I is the loss modulus, G" (the viscous portion), and tan δ is a mechanical damping or internal friction, i.e. tan δ = G"/G', sin δ = G"/G*, and G* = G' + i G". If the isochronal sin δ is one, the system is considered a Newtonian fluid, i.e. the storage modulus vanishes since sin $\delta \cong 1$, G*/sin $\delta \cong$ G".

The isochronal sin δ curves are a function of temperature for asphalt/polymer blends as illustrated in figures 25 and 26. In figure 25, all of these curves approach unity at high temperatures as the visco-elastic fluids begin to flow as Newtonian fluids. In other words, there was no elasticity (i.e., G' = 0) either in original or aged asphalt binders at high temperatures. The polymer particles do not interfere with the measurement. However, figure 26 shows that the sin δ of blends with CPE curves are substantially less than one, even at temperatures above the melting point of the asphalt matrix. All isochronal sin δ curves of blends with CPE, as illustrated in figure 26, approached unity at higher temperatures as the viscoelastic fluids began to flow. A sin δ of unity confirms that the flow of an asphalt ACL-2 is Newtonian at temperatures equal to or greater than 64°C. However, the sin δ of the CPE/asphalt blend curve is substantially less than one at 64°C. This indicates that CPE modified ACL-2 is not Newtonian, even at high temperatures. The chlorinated HDPE exhibits good interaction with the polar fractions of asphalt cement. Clearly, the polymer additive contributes to the visco-elastic properties in the CPE modified ACL-2 binders over a wide temperature range. One would expect this interaction to improve high temperature pavement performance. As expected, the deviation from Newtonian flow increases as the binder is aged. The increased visco-elastic properties in ACL-2/CPE binders at higher temperatures should improve pavement performance at the maximum reference temperature.

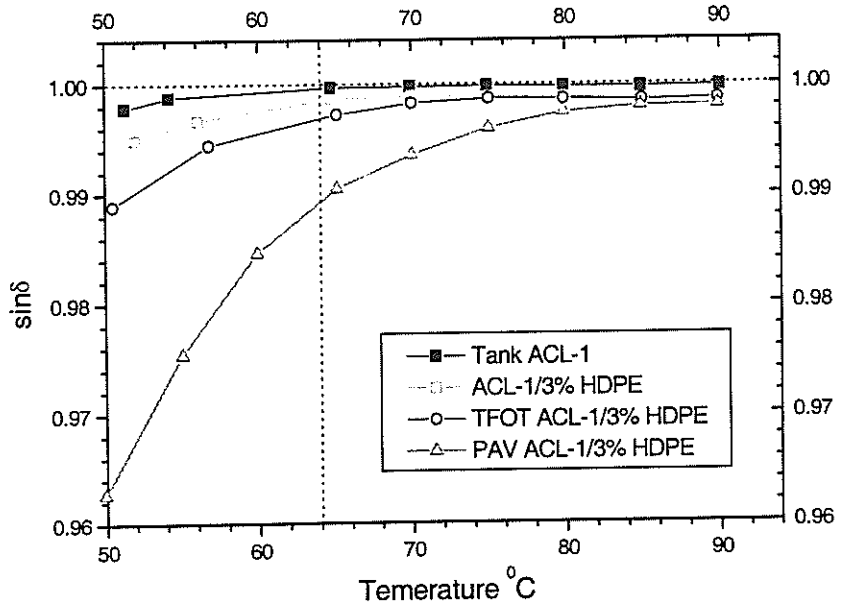

Figure 25
Variation of sin δ with temperature for a blend of ACL-1 with 3 percent HDPE. Dotted lines are set at sin δ = 1.0 and T= 64°C

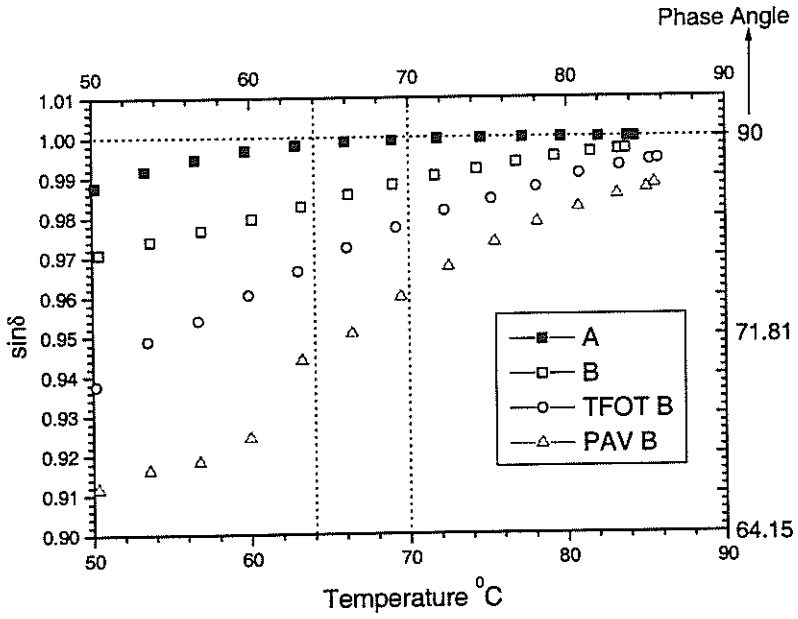

Figure 26
Variation of sin δ with temperature for A: ACL-2 and B: CPE modified ACL-2. Dotted lines are set at sin δ = 1.0, T= 64°C, and 70°C, respectively

In Superpave PG asphalt specifications, the stiffness parameter, G*/sin δ, was selected to express the contribution of the asphalt binder to permanent deformations. This value reflects the total resistance of a binder to deformation under repeated loading (G*) and the relative amount energy dissipated into non-recoverable deformation (sin δ) during a loading cycle. Higher values of the parameter rate are expected to result in high resistance to permanent deformation. The G*/sin δ value should be larger than 1000 Pa at 10 rad/s for the original binder at a maximum pavement design temperature. Isochronal plots of G*/sin δ reveal distinct differences due to the modifier's ability to mix with asphalt (figure 27). Both of the modified asphalts are qualified according to SHRP specifications of the stiffness parameter at 64°C. However, only the blends containing chlorinated HDPE meet the SHRP specification at 70°C. The introduction of chlorine atoms enhances compatibility between the polymer additives and asphalt, and the volume of the polymer rich phase will be increased due to improved "solubility" in the asphalt. As a result of the enhanced solubility, the sin δ remains less than unity at the higher temperature. This phenomenon raises the value of the G*/sin δ ratio and the maximum qualifying temperature for the blend. Obviously, the increases are significant and are expected to result in improved pavement resistance to rutting when the pavement is open for service.

The dynamic shear rheometer measurements for each of the blends prepared in this study are summarized in table 8. The data for the original binder was recorded at the maximum reference temperature where the G*/sin δ ratio exceed 1.0 kPa. The impact of TFOT aging was examined by determining the G*/sin δ ratio at the same reference temperature.

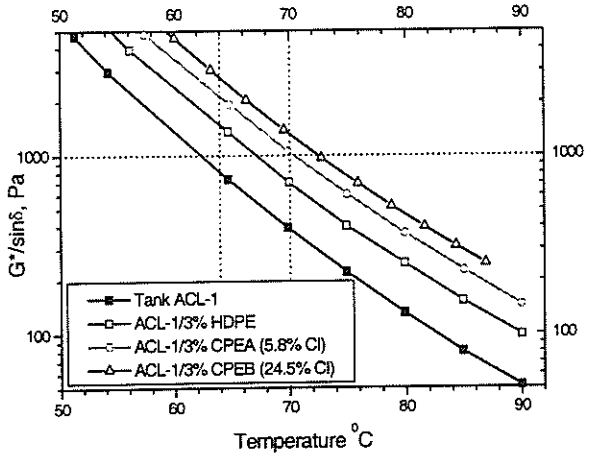

Figure 27
Comparison between rutting factors (G*/sin δ) of tank asphalt and blends with HDPE or chlorinated HDPE. Dotted lines are set at Superpave PG qualifying values of 1.0 KPa, 64°C, and 70°C, respectively

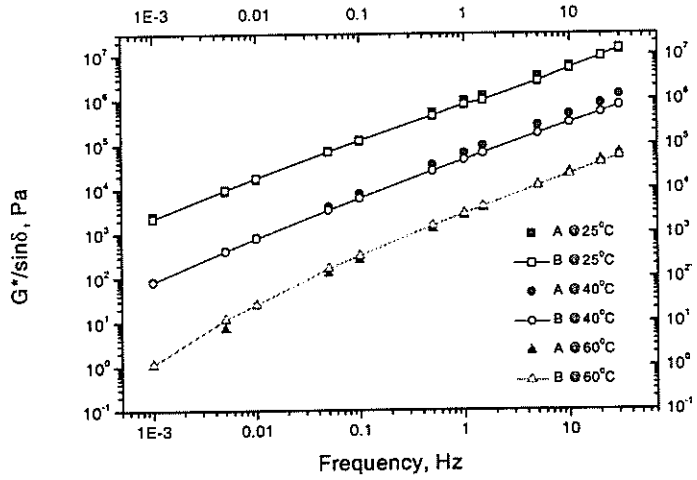

Figure 28
Comparison between G*/sin δ vs. frequency at 25°C, 40°C and 60°C; A, ACL-2; B, CPE modified ACL-2

Table 8

Summary of dynamic shear rheometer test results on polymer modified asphalt blends, Superpave PG criteria: original binder, G*/sin δ ≥ 1.0 kPa, TFOT-aged binder, G*/sin δ ≥ 2.2 kPa, PAV-aged binder, G*sin δ ≤ 5,000 kPa

Sample	% Add	Original Binder G*/sin δ, kPa	TFOT-aged Binder G*/sin δ, kPa	PAV-aged Binder G*sin δ, kPa
ACL-1	0	2.0 @58°C or 0.8 @64°C	7.6 @58°C or 2.8 @64°C	43.5 @22°C
ACL-1/HDPE	3	1.4 @64°C	2.8 @64°C	2500 @25°C
ACL-1/CPEA	3	1.9 @64°C	3.7 @64°C	2700 @25°C
ACL-1/CPEB	3	2.8 @64°C	3.4 @64°C	778 @25°C
ACE-1	0	1.0 @64°C	2.7 @64°C	4028 @28°C
ACE-1/HDPE	3	1.6 @64°C	3.4 @64°C	1600 @25°C
ACE-1/CPEA	3	1.7 @64°C	10 @64°C	1700 @25°C
ACE-3	0	1.4 @64°C	4.1 @64°C	2356 @25°C
ACE-3/SBS (PAC40)	3	1.8 @70°C	3.2 @70°C	983 @28°C
ACM-3	0	1.1 @70°C	2.7 @70°C	820 @31°C
ACM-3/HDPE	3	2.1 @70°C	2.7 @70°C	947 @31°C
ACM-3/CPEA	3	2.1 @70°C	3.5 @70°C	817 @31°C
ACR-3	0	1.0 @70°C	6.6 @70°C	727 @31°C
ACR-3/HDPE	3	1.7 @70°C	2.7 @70°C	899 @31°C
ACR-3/CPEA	3	1.8 @70°C	3.1 @70°C	813 @31°C
ACR-3/MPP	3	2.9 @70°C	3.5 @70°C	1562 @28°C
ACR-3/MPPPVA	3	2.5 @70°C	2.6 @70°C	2134 @28°C
ACR-3/MPPEAH	3	1.7 @70°C	2.2 @70°C	1761 @28°C
ACR-3/MPPNA	3	2.9 @70°C	3.2 @70°C	2527 @28°C
AAD-1	0	1.3 @64°C	3.5 @64°C	1148 @25°C
ABC-1	0	1.3 @70°C	2.3 @70°C	823 @28°C

In order to evaluate the permanent deformation (rutting) and the fatigue cracking of aged asphalt binders, the Superpave PG specifications require determination of G* sin δ (or G") for TFOT and PAV aged materials. The permanent deformation is related to the ratio G*/sin δ, which must be at least 2.2 kPa after TFOT aging at specified high temperatures. The product of G*sin δ (or G") is represented as a fatigue cracking factor in asphalt pavements, i.e. a maximum limit of 5,000 kPa at average service temperatures is set in the Superpave PG asphalt specifications. The ability to dissipate or relax stress is a desirable binder character in resisting fatigue cracking. An inspection of the data in table 8 shows that there is no significant difference between tank ACL-1 and ACL-1/HDPE in TFOT stage, i.e., the same G*/sin δ value is observed at 64°C either in tank ACL-1 or ACL-1/HDPE. This observation suggests that gross phase separation occurs after the thin film aging of the ACL-1/HDPE blend, which could result in the same rheological properties as unmodified asphalt. The

G*/sin δ of ACL-1/CPE blends were somewhat higher than the aged tank asphalt. Thus only partial phase separation occurred in this blend at high temperatures. However, all of the PMAC's met the qualification SHRP at 64°C.

Note in figure 28 that there is little difference between the G*/sin δ vs. frequency plots for ACL-2 and CPE modified ACL-2. However, at 40°C, the values for G*/sin δ of ACL-2 begin to exceed those of the CPE modified binder. The ACL-2 behaves as a stiffer mix at higher frequencies. The presence of CPE in the binder allows the matrix to respond to deformations and should favor low temperature cracking resistance.

On the other hand, tests on fatigue cracking for PAV asphalt binders, as illustrated in figure 29, show that the products of complex modulus (G*) times sin δ for both the PAV aged ACL-1/HDPE and ACL-1/CPEA blends are less than that of PAV aged tank asphalt at all temperature ranges. Extrapolation of the data to the temperature at which G*sin δ reaches 5,000 kPa illustrates this point. The extrapolated temperature for ACL-1/HDPE or ACL-1/CPEA is much lower than that of the aged tank sample. The G*sin δ values of the PAV aged blends examined in this study are summarized in table 8. The data are reported for the blend at the Superpave qualifying temperature.

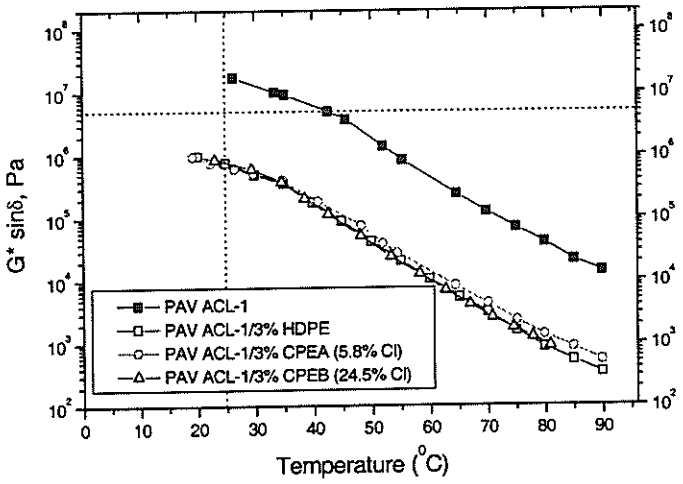

Figure 29
Variation of G*sin δ with temperature for tank asphalt and of blends with HDPE or chlorinated HDPE. Dotted lines are set for Superpave PG qualifying value of 5,000 kPa at 25°C

Low-Temperature Creep Response of Asphalt Binder

Preliminary low temperature creep properties of asphalt blends using bending beam rheometer can be obtained by knowing the creep load applied to the beam and the deflection at several loading times during the test. The creep stiffness can be calculated using engineering beam mechanics. According to the Superpave protocol, the stiffness (S(t)) and creep rate of the binder under load ($m = \left| d \log S(t) / d \log(t) \right|$) are reported at specification temperatures after a 60 second loading period, which simulates stiffness after two hours at 10°C lower temperature. The data were collected at -12°C, and, as limits for this test, the SHRP specifications were $S(t = 60) \leq 300$ MPa and m-value (slope) ≥ 0.3. It is expected that binders with high creep stiffness will crack at low temperatures. Likewise, binders with high m-values are more effective in shedding stresses that build in asphalt pavements as temperatures drop, ensuring that low temperature cracking will be minimized. The data in figure 30 indicate that all asphalt binders met the S(t) and m-value performance criteria for the chosen temperature, (-12°C).

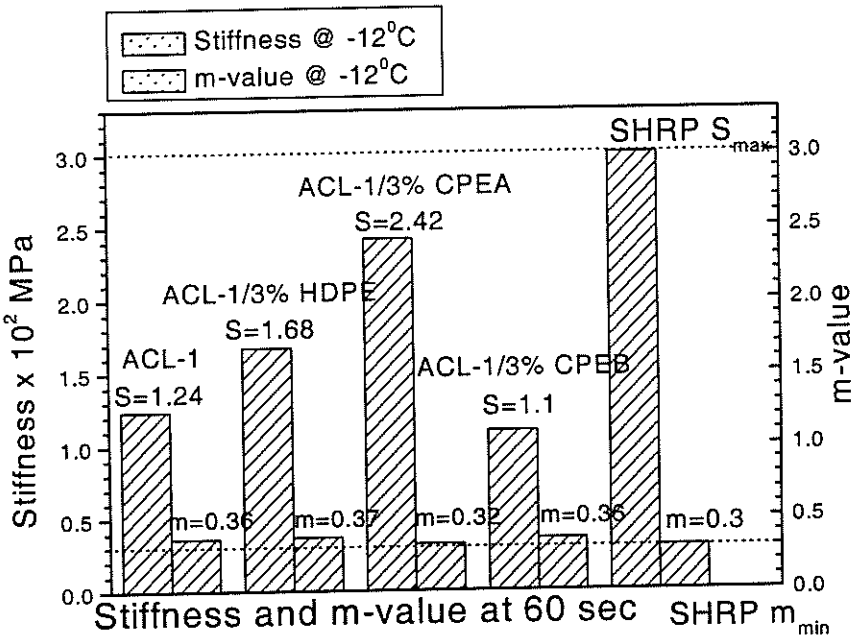

Figure 30
Creep stiffness of PAV aged ACL-10 blends containing HDPE and chlorinated HDPE. Dotted lines are set at Superpave PG qualifying values of 300 MPa, m = 0.3

Table 9

Influence of asphalt type and polymer type on low-temperature creep response and their PG grading and Superpave PG standard, stiffness ≤ 300MPa, m-value ≥ 0.30

Sample	% Add	Stiffness(MPa) @-12°C	m-value	PG Grading
ACL-1	0	124	0.36	58-22
ACL-1/HDPE	3	168	0.37	64-22
ACL-1/CPEA	3	242	0.32	64-22
ACL-1/CPEB	3	110	0.36	64-22
ACE-1	0	384	0.29	64-16
ACE-1/HDPE	3	163	0.37	64-22
ACE-1/CPEA	3	169	0.34	64-22
ACL-2	0	170	0.32	64-22
ACL-2/CPEB	3	127	0.33	70-22
ACE-3	0	173	0.35	64-22
ACE-3/SBS (PAC40)	3	110	0.39	70-22
ACM-3	0	122	0.34	70-22
ACM-3/HDPE	3	450	0.26	70-16
ACM-3/CPEA	3	375	0.30	70-16
ACR-3	0	333	0.30	70-16
ACR-3/HDPE	3	391	0.30	70-16
ACR-3/CPEA	3	460	0.30	70-16
ACR-3/MPP	3	221	0.33	70-22
ACR-3/MPPPV	3	210	0.34	70-22
ACR-3/MPPEA	3	189	0.36	70-22
ACR-3/MPPNA	3	212	0.33	70-22

In a typical dynamic mechanical analysis (DMA), the tan δ (tan δ = E"/E', where E" and E' are the loss modulus and the storage modulus, respectively, in the relation giving the complex modulus of elasticity E*, viz., E* = E' + iE") for films of ACL-2 and CPEB modified ACL-2 is plotted in figure 31. The plot for ACL-2 exhibits definite peaks associated with the Tg of asphalt components at temperatures between -10°C and -30°C. These peaks were practically eliminated by blending the asphalt with three percent CPEB, suggesting a plasticizing effect of the polymer, or in other words, a depression of the Tg domain to lower temperatures. These results are well correlated with the BBR data for the same temperature domain, which indicated a lower stiffness (S) and a corresponding slightly higher creep rate (m) for CPE modified ACL-2 as compared to ACL-2 (shown in table 9).

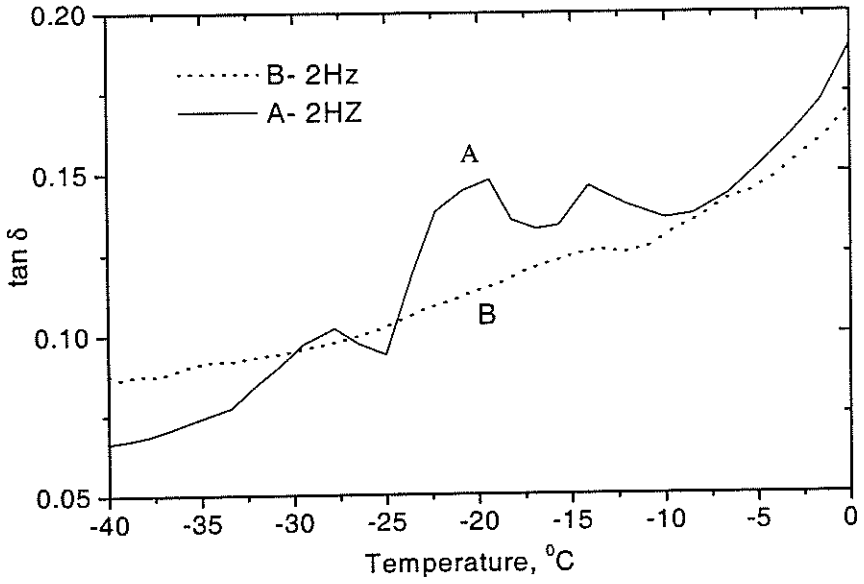

Figure 31
Comparison between tan δ at lower temperatures for A: ACL-2 and B: CPEB modified ACL-2 (film measured at 2Hz)

The creep and recovery measurements provide rheological data characteristic of the particular binder under conditions employed. Thus, this method allows one to simulate the response of road covering materials when they are subjected to temporary loads. The constant stress creep/creep recovery test (figure 32) illustrates a significant difference between the deformation of CPE and HDPE blends. This observation might be an indication of their rutting resistance (i.e., the lower the deformation, the better the binder response to rutting), which is related to the composition of the asphalt binder. The ACL-1/CPE material has much more resistance to creep than ACL-1/HDPE or pure asphalt at 50°C. Therefore, it would be expected to yield better material with the maximum rutting resistance that can be imparted by the binder.

Creep testing gives an indication of the resistance of the asphalt binder to deformation, while the recovery percentage gives an indication of the elastic resilience of the asphalt binder. Elastic creep recovery of asphalt samples can be observed in figure 33 after the stress was removed. As expected, blends containing the additive prepared by modification of HDPE by chlorination exhibited significantly less creep and higher creep recovery than a corresponding HDPE blend. This is due to the presence of the more elastic filler. On the

other hand, the pure asphalt sample did not display any recovery, and the presence of HDPE in asphalt did not improve recovery percentage under these conditions.

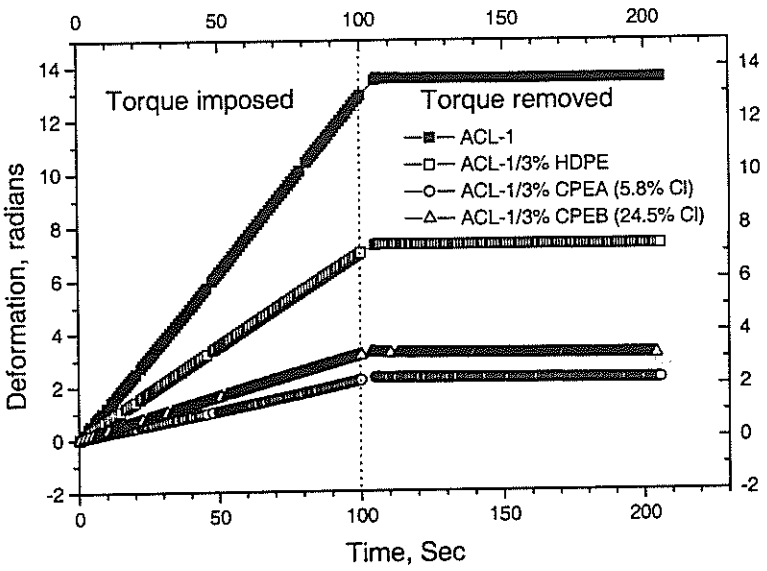

Figure 32
Constant stress creep/creep recovery curves at 50°C of ACL-1 blends with HDPE or CPE

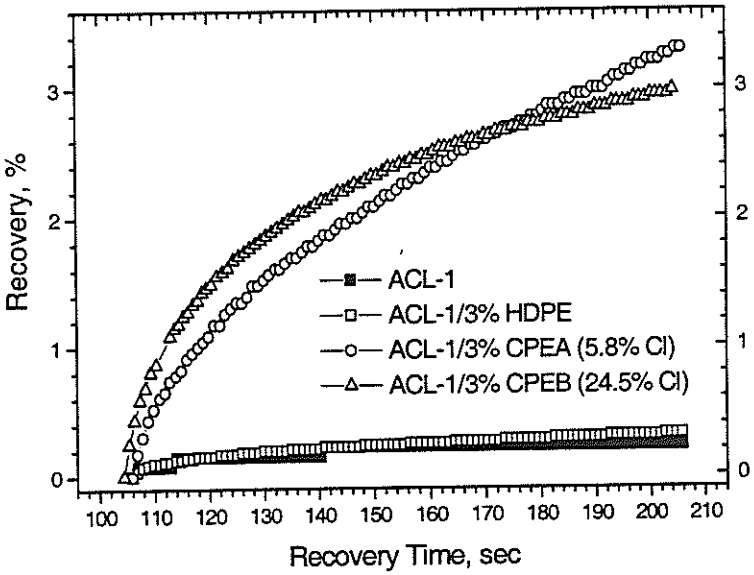

Figure 33
Extent of percent recovery curves of ACL-1 blends containing HDPE or CPE at 50°C

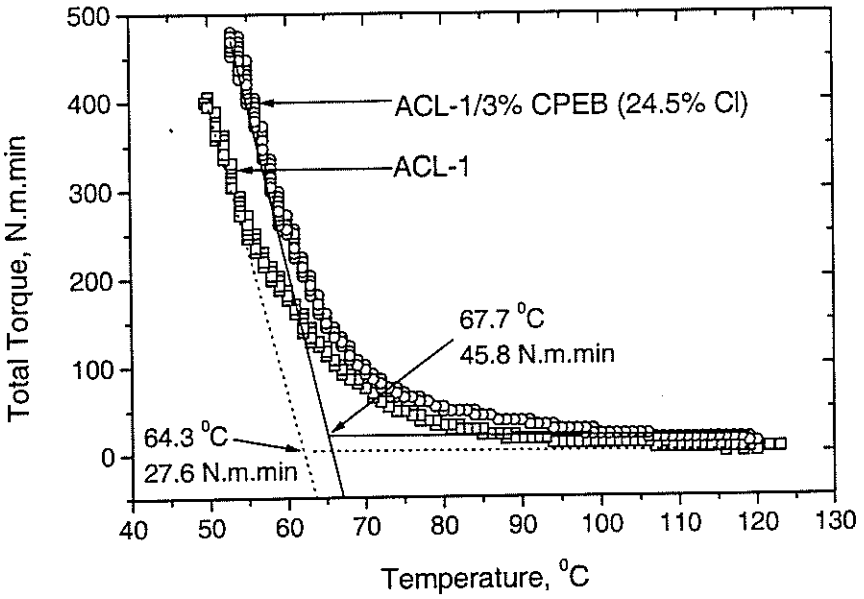

Figure 34
Total torque vs. temperature on cooling asphalt blends

Table 10
Summary of constant stress creep/creep recovery test results at 100 Pa, 0.25mm, and 50°C

Sample	% Add	Deformation (radians) @ 100 sec	% Recovery
ACL-1	0	13	0.2
ACL-1/HDPE	3	7	0.3
ACL-1/CPEA	3	2	3.3
ACL-1/CPEB	3	3	3.0
ACL-2	0	2.5	0.3
ACL-2/CPEB	3	5.5	1.8
ACE-1	0	2	0.2
ACE-1/HDPE	3	6	1.0
ACE-1/CPEA	3	5	1.2
ACM-3	0	26	0.6
ACM-3/HDPE	3	11	8.6
ACM-3/CPEA	3	15	1.8
ACR-3	0	21	0.1
ACR-3/HDPE	3	0.1	-
ACR-3/CPEA	3	0.9	2.1

The viscosity-related total torque of both tank asphalt and asphalt blend during cooling under agitation is clearly revealed in figure 34. There are no differences in the total torque required to mix either tank ACL-1 or ACL-1/3 percent CPEB at high temperatures. However, when the sample temperature reached 70°C, the crystallization temperature of the CPE employed, a rapid increase in the total torque was observed, indicating that the polymer was contributing significantly to the viscosity of the mixture. This observation confirms that phase separation does not occur on cooling for the ACL-1/3 percent CPEB blend when a high degree of chlorination is employed.

Indirect Tensile Strength and Strain Test

The influence of CPE-modified asphalt on the ITS and the strain of the studied asphaltic concrete mixtures is presented in figure 35. Desirable HMAC mix properties are a high tensile strength and strain at failure, though there are no specific limits defined for these engineering properties. It appears that the indirect tensile strength of CPE-modified asphalt mix (C20 mix) is significantly higher than the tank asphalt mix (A20 mix) at 25°C; however, the indirect tensile strain at failure of the C20 mix is not significantly different than the A20 mix. It is interesting to note that the increase in the ITS of the C20 mix did not show any significant decrease in the corresponding tensile strain. This observation is supported by the value of G*sin δ reported in table 1. Table 11 shows the mean ITS and strain along with their standard deviation and coefficient of variation.

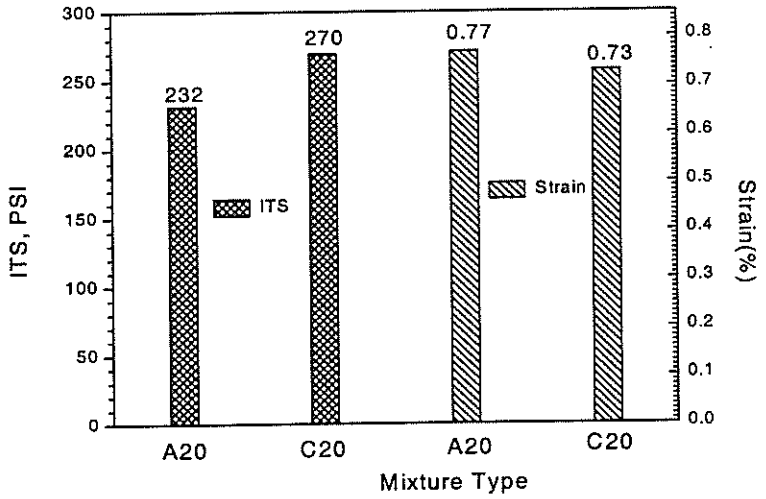

Figure 35
Indirect tensile strength and strain test results at 25°C

Table 11
Statistical grouping of indirect tensile strength and strain test results

Property	ITS, psi		Strain %	
Mix Type	A20	C20	A20	C20
Mean	232	270	0.77	0.73
STD	11	10	0.05	0.13
CV%	4.8	3.6	6.5	17
Group	*B*	*A*	*A*	*A*

Indirect Tensile Resilient Modulus Test

Mean values, standard deviations, and coefficients of variation, along with their statistical grouping, are compiled in table 12 for total M_R tests results at three temperatures: 5°C, 25°C, and 40°C. A high resilient modulus for a HMAC is desirable to achieve a better resistance to permanent deformation at high service temperatures. On the other hand, a high strain tolerance is desired to resist cracking caused by load stress and thermal stresses within the HMAC at low temperatures. As expected, the resilient modulus value decreased, increasing the temperature for both mixes. However, CPE modified mixes exhibited significantly higher stiffness than the corresponding mixes with ACL-2 (figure 36). CPE modified mix presented significantly higher stiffness at 40°C than the ACL-2 mix. These results are consistent with the corresponding binder rheology. It is also interesting to note that the CPE modified mixes possessed significantly higher M_R values than the ACL-2 mixes at low temperatures. However, the binder rheology indicates that the low temperature CPE addition did not effect the low temperature properties, as measured from the BBR m-value (table 9). The high temperature behavior can be supported by the higher elastic recovery characteristics of the CPE modified ACL-2 as illustrated in table 10.

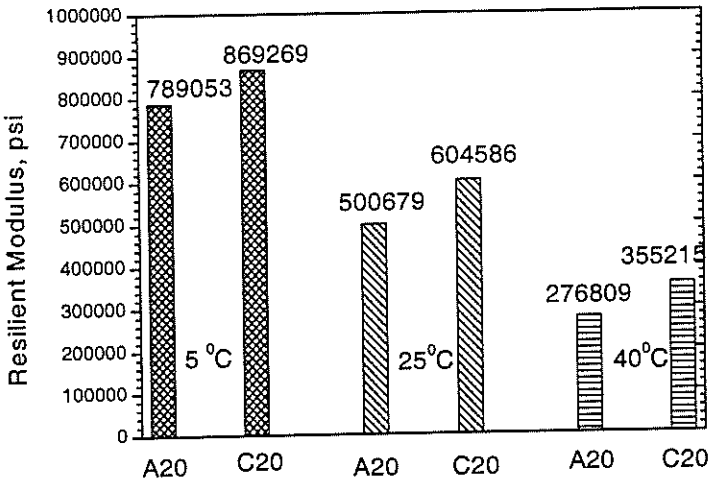

Figure 36
Comparison between resilient modulus of A20 and C20 mixes at 5°C, 25°C, and 40°C

Table 12
Statistical grouping of indirect tensile resilient modulus test results

Mix type		A20				C20			
	TEMP(°C)	MEAN	STD	CV%	Group	MEAN	STD	CV%	Group
M_R, psi	5	789053	65599	8	B	869269	95168	11	A
	25	500679	29675	6	B	604586	37467	6	A
	40	276809	14802	5	B	355215	17168	5	A

M_R: Resilient Modulus, psi

Indirect Tensile Creep Test

The results of the G*/sin δ indirect tensile creep slope and time to failure for the two mixes are presented in figure 37 and table 13. This test is conducted to evaluate the rutting susceptibility of the asphaltic concrete mixes. A low creep slope value and long times to failure are desirable properties. The mixture containing the CPE modified binder had a lower creep slope than the mixture containing ACL-2; however, the decrease was not significant. The times to failure of CPE modified mixes were significantly higher than those with ACL-2 binders. In general, the addition of CPE to ACL-2 improved the mixture's resistance to rutting. A lower value of G*/sin δ for CPE modified ACL-2 might be misleading in terms of

the rutting resistance if one does not also consider the variation of the phase angle with temperature (figure 26). A lower phase angle indicates a binder with higher elastic component. There is an increased resistance to mixture permanent deformation as observed by this test.

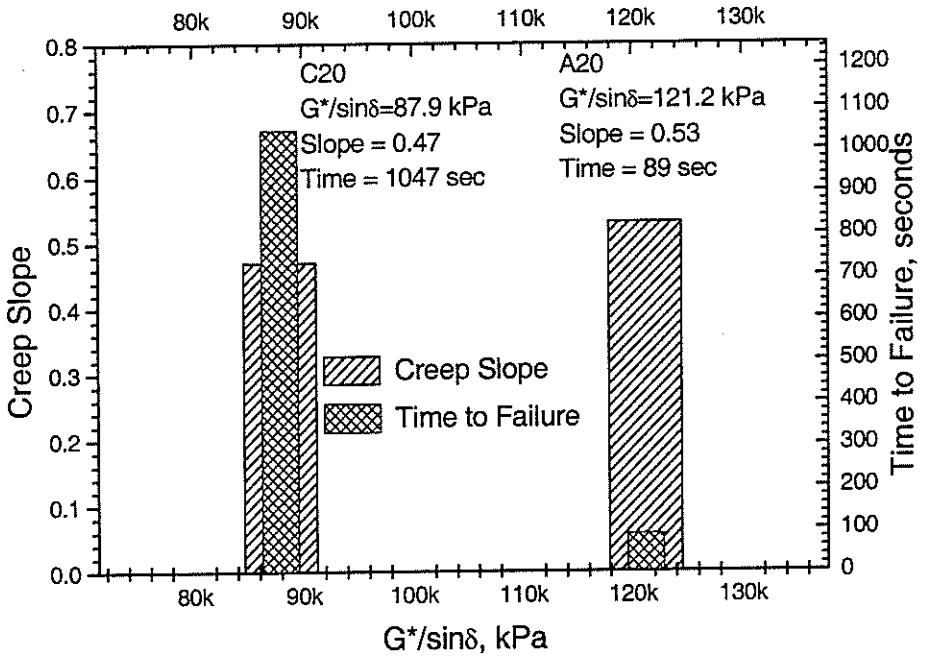

Figure 37
Comparison between creep slope and time to failure of A20 and C20 mixes at 40°C

Table 13
Statistical grouping of indirect tensile creep test results at 40°C

Property	Creep Slope		Time to Failure (sec)	
Mix Type	A20	C20	A20	C20
Mean	0.53	0.47	89	1047
STD	0.03	0.04	19	321
CV%	6	9	22	31
Group	*A*	*A*	*B*	*A*

Indirect Tensile Fatigue Test

Table 14 and figure 38 present a summary of the mixture fatigue test results and corresponding binder rheology (G*sin δ). The properties obtained from this test are the number of cycle times to failure, N_f, and the fatigue slope. Fatigue slope is the rate of change in permanent deformation with an increased number of cycles. Desirable properties for a high fatigue endurance mix are low fatigue slope value and high number of cycles to failure for an asphaltic concrete mixture. The addition of CPEB to ACL-2 has not improved fatigue slope significantly but has greatly increased the number of cycles to failure (table 14). Also, the fatigue mix properties (slope and N_f) correlate to the binder rheology, G*sin δ, as shown in figure 38.

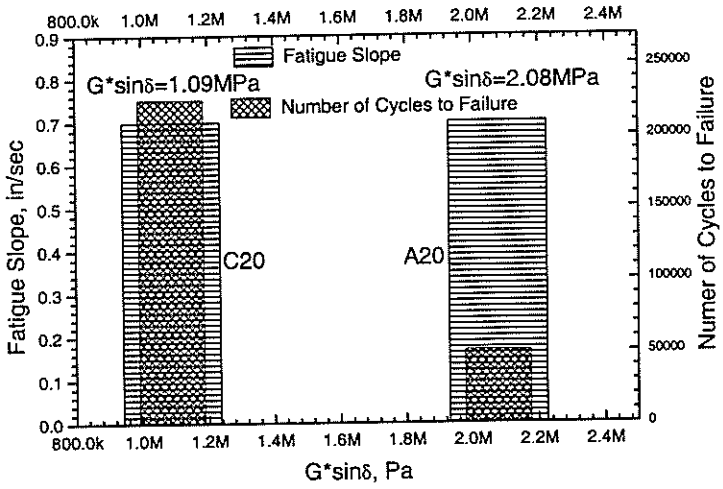

Figure 38
Comparison between fatigue factors of asphalt binders and their HMAC at 25°C

Table 14
Statistical grouping of indirect tensile fatigue test results at 25°C

	Fatigue Slope (Power Fit)		Number of Cycles to Failure	
	A20	C20	A20	C20
Mean	0.70	0.66	51130	225513
STD	0.06	0.37	19854	34646
CV%	8.2	5.6	38.8	15.4
Group	*A*	*A*	*B*	*A*

CONCLUSIONS

Asphalt modification using polymeric additives, including chlorinated and maleated polyolefins as well as unmodified polyolefin such as PE, have been reported in this study. Chlorination of HDPE can be controlled to produce semi-crystalline polymeric additives, depending upon the degree of chlorination achieved. The results of the studies showed that introducing chlorine atoms on HDPE chains can improve compatibility of the asphalt/polymer blends through adjusting the interaction between the components of asphalt and polymer. The chlorine content in HDPE affects the phase structure of the asphalt blends, which leads to better performance in asphalt blend compatibility. Maleation of polyolefins at very low levels (one to two percent) is an effective means for enhancing the polarity of the additive without influencing the degree of crystallization. The more polar additives also produce compatible polymer/asphalt blends.

DSC can be used as tool for determining the asphalt crystallinity and the distribution components among phases in asphalt/polymer blends. The crystallization process of the asphalt binder depends on heavily on time. To enhance the resolution of a given thermogram, a several step annealing process is required to experimentally realize a near-equilibrium state. DSC measurements on annealed samples reveal more thermal transitions than those observed with tank asphalts.

A study was conducted to examine the feasibility of using waste materials converted to CPE as modifiers to paving grade asphalt. Both a binder rheology study and a mixture characterization were conducted to compare the performance of conventional dense graded mix containing ACL-2 and CPE modified ACL-2. In general, the addition of CPE has improved the mix properties as measured from the indirect tensile strength tests, indirect resilient modulus test, indirect creep test, and fatigue test. Also, binder rheology correlated well with mix properties. Specific observations include:

1. All of the ACL-2 asphalt binders exhibit the viscosity (η) at 135°C less than 3.0 Pa·s. The ratio of viscosity increases upon aging, PAV/original, for ACL-2 and CPE modified ACL-2, was much less for the polymer modified binder (i.e. 3.1 and 2.2, respectively). This observation suggests that the polymer additive protects the asphalt matrix from age hardening.

2. The sine of the phase angle, sin δ, is a good indicator for the flow behavior of the asphalt binders. ACL-2 lost its elastic component at $T \cong 60°C$ when $\sin \delta \cong 1.00$. However, CPE modified ACL-2 maintained an elastic component even at $T > 70°C$ ($\sin \delta < 1.0$, $G' \neq 0$).
3. The binder contribution to permanent deformation resistance, as reflected by creep and creep recovery, can be enhanced by polymer additives. These tests may directly relate to the compatibility of a polymer modifier in asphalt cement at high temperatures. The elastic recovery of asphalt cements is improved by the addition of CPE.
4. The low-temperature cracking properties of asphalt binders can be estimated by three-point bending studies. PAV aging of the asphalt/CPE blend revealed the highest creep stiffness and the lowest creep rate compared to tank asphalt and asphalt/HDPE.
5. DSC can be used to evaluate the endothermic transitions from the melting/dissolution of crystalline and amorphous regions of blends. The flow behavior depends on the distribution of asphalt components among phases in asphalt/polymer blends.
6. The rutting resistance of the blends, as reflected by $G^*/\sin \delta$, can be enhanced depending upon the nature of the polymer additive and the degree of age hardening in binders. These tests directly reflect the compatibility of a polymer modifier on asphalt cement at high temperatures.
7. Blends of chlorinated polyolefins with asphalt are more compatible than the corresponding blends with simple polyolefins. The polymer additive appears to protect the asphalt matrix from age hardening and could extend the lifetime of the corresponding asphalt cements.
8. The CPE-modified HMAC mix demonstrated improving fundamental engineering properties at all temperatures.

Recommendations

Future studies should apply polyimide chemistry to the design of additives with specific enhancement properties, i.e., improved strip resistance. In addition, surface energy of both polymeric additives and asphalts should be determined in order to gain a better understanding of the compatibility between polymer and asphalt. Briquettes of asphalt cements based on conventional ACL-2 and CPE modified ACL-2 have been prepared and investigated. Future studies should focus on the effects of other mix variables on the performance of HMAC such as void content, nominal maximum aggregate sizes, aggregate source, and the compaction levels. Also, the effect of the moisture susceptibility behavior of HMAC with anti-stripping additives should be evaluated. The future complete implementation of HMAC in practice to undertake a full range of standard and specialized tests should be expanded to include the loaded wheel test from the asphalt pavement analyzer (APA), indirect tensile tester, and Superpave shear tester (SST). The same preparation and testing protocol, and the fundamental engineering properties of HMAC containing conventional and MPP modified asphalt cements should be explored.

ACRONYMS/ABBREVIATIONS/SYMBOLS

λ	Wave length
μ	Poisson Ratio
η	Viscosity
ΔH_f	Heat of fusion
ΔH_T	Total recoverable horizontal deformation
ΔV_T	Total recoverable vertical deformation
ΔV (t)	Vertical deformation at time t
AASHTO	American association of state highway and transportation officials
AC	Asphalt Cement
ASTM	American society for testing and materials
BBR	Bending Beam Rheometer
BC	Binder Course
C	Celsius
C(t)	Creep modulus
CI	Carbonyl Index
CPE	Chlorinated Polyethylene
CS	Coarse Sand
DCB	Dichlorobenzene
DCP	Dicumyl Peroxide
DMA	Dynamic Mechanical Analysis
DMS	Dynamic Mechanical Spectrometer
DSC	Differential Scanning Calorimetry
DSR	Dynamic Shear Rheometer
ESEM	Environmental Scanning Electron Microscope
EVA	Ethylene-Vinyl Acetate Copolymer
FS	Fine Sand
FTIR	Fourier Transform Infrared
G*	Shear complex modulus
G′	Shear storage modulus
G"	Shear loss modulus
GTM	Gyratory testing machine

HDPE	High Density Polyethylene
PE	Polyethylene
HMAC	Hot Mix Asphalt Concrete
Hz	Hertz
ITS	Indirect Tensile Strength
JMF	Job Mix Formula
L	Liter
LADOTD	Louisiana Department of Transportation and Development
LCR	Large Crushed Gravel
LDPE	Low Density Polyethylene
LTRC	Louisiana Transportation Research Center
LVDT	Linear Variable Differential Transformers
m	Creep rate under load
MAH	Maleic Anhydride
MI	Melt Index
MIM	Miniaturized Internal Mixer
MPP	Maleated Polypropylene
MPPAM	Modification of Maleated Polypropylene with N-amino-morpholine
MPPEA	Modification of Maleated Polypropylene with Ethanolamine
MPPNA	Modification of Maleated Polypropylene with, 1-Naphthylamine
M_R	Indirect tensile resilient modulus
MTS	Material Testing System
N_f	Number of cycle times to failure
NMR	Nuclear Magnetic Resonance
Pa·s	Pascal
PAV	Pressure Aging Vessel
PMAC	Polymer Modified Asphalt Cement
P_o	Applied vertical load
PP	Polypropylene
P_{ULT}	Ultimate applied load to failure
PVA	Polyvinyl Alcohol
rad	Radian
RV	Rotational Viscometer
s	Second
S(t)	Creep stiffness
SAH	Succinic Anhydride

SAS	Statistical Analysis System
SBS	Styrene-Butadiene-Styrene Block Copolymer
SHRP	Strategic Highway Research Program
STD	Standard Deviation
Superpave™	Superior performance asphalt pavements
TBPB	t-Butyl Perbenzoate
TCE	1, 1, 2, 2-tetrachloroethane
TEPA	Triethyl Phosphate
TFOT	Thin Film Oven Test
Tg	Glass transition temperature
Tm	Melting point
Tr	Transition temperature
TS	Percent Tensile Strain
VFA	Volume of Voids Filled with Asphalt
VMA	Volume of Voids in Mineral Aggregate

REFERENCES

1. Stewart, L., "Polymers: Pavement's Miracle Additive", *Highway & Heavy Construction*, Vol. 132, No. 13, 1989, pp 48-50.

2. King, G.N., Harders, O., and Chavenot, P., "Influence of Asphalt Grade and Polymer Concentration on the High Temperature Performance of Polymer Modified Asphalt", *Proceedings of the Association of Asphalt Paving Technologists*, Vol. 61, 1992, pp. 29-66.

3. Goodrich, J.L., Goodrich, J.E., and Kari, W.J., "Asphalt Composition Tests: Their Application and Relation to Field Performance", *Transportation Research Record*, Vol. 1096, 1985, pp. 146-167.

4. Petersen, J.C., Robertson, R.E., Branthaver, J.F., Harnsberger, P.M., Duvall, J.J., Kim, S.S., Anderson, D.A., Christiansen, D.W., Bahia, H.U., Dongre, R., Antle, C.E., Sharma, M.G., Button, J., and Glover, C.J., "Binder Characterization and Evaluation: Test Methods", SHRP-A-370, Strategic Highway Research Program, National Research Council, Washington, D. C., 1994, p. 193.

5. Daly, W.H., Qiu(Chiu), Z.-Y., and Negulescu, I.I., "Differential Scanning Calorimetry Study of Asphalt Crystallinity", *Transportation Research Record*, Vol. 1535, 1996, pp. 54-60.

6. Noel, F. and Corbett, L.W., "A Study of the Crystalline Phases on Asphalt", *J. Inst. Petrol.* Vol. 56, No. 551, 1970, pp. 261-265.

7. Huynh, H.K., Khong, T.D., Malhotra, S.L., and Blanchard, L.P., "Effect of Molecular Weight and Composition on the Glass Transition Temperatures of Asphalts", *Analytical Chemistry*, Vol. 50, No. 7, 1978, pp. 976-979.

8. Brule, B., Planche, J.P., King, G.N., Claudy, P., and Letoffe, J.M., "Relationships Between Characterization of Asphalt Cements by Differential Scanning Calorimetry and Their Physical Properties", *Prepr. Am. Chem. Soc., Div. Pet. Chem.*, Vol. 35, No.3, 1990, pp. 330- 337.

9. Claudy, P., Brule, B., Planche, J.P., King, G.N., and Letoffe, J.M., "Characterization of Paving Asphalts by Differential Scanning Calorimetry", *Fuel Science and Technology Int'l.*, Vol. 9, No. 1, 1991, pp. 71-92.

10. Claudy, P., Planche, J.P., King, G.N., and Letoffe, J.M., "Characterization of Asphalts by Thermomicroscopy and Differential Scanning Calorimetry: Correlation to Classic Physcial Properties", *Fuel Science and Technology Int'l.*, Vol. 10, No. 4-6, 1992, pp. 735-765.

11. Brule, B., Brion, Y. and Tanguy, A., "Paving Asphalt Polymer Blends: Relationships Between Composition, Structure and Properties", *Proceedings of the Association of Asphalt Paving Technologists*, Vol. 57, 1988, pp. 41-64.

12. Collins, J.H., Bouldin, M.G., Gelles, R., and Berker, A., "Improved Performance of Paving Asphalts by Polymer Modification", *Proceedings of the Association of Asphalt Paving Technologists*, Vol. 60, 1991, pp. 43-69.

13. King, G.N., Muncy, H.W., and Prudhomme, J.B., "Polymer Modification: Binder's Effect on Mix Properties", *Proceedings of the Association of Asphalt Paving Technologists*, Vol. 55, 1986, pp. 519-540.

14. Collins, J.H. and Mikols, W.J., "Block Copolymer Modification of Asphalt Intended for Surface Dressing Applications", *Proceedings, Association of Asphalt Paving Technologists*, Vol. 54, 1985, pp. 1-13.

15. Coyne, L.D., "Evaluation of Polymer Modified Chip Seal Coats", *Proceedings, Association of Asphalt Paving Technologists*, Vol. 57, 1988, pp. 545-575.

16. Jew, P. and Woodhams, R.T., "Polyethylene-Modified Bitumens for Paving Applications", *Proceedings, Association of Asphalt Paving Technologists*, Vol. 55, 1986, pp. 541-559.

17. Hesp, S.A. and Woodhams, R.T., *Polyolefin-Asphalt Emulsions*, in *ASTM STP 1108*, K.R. Wardlaw and S. Schuler, Editors. 1991: Philadelphia, PA.

18. Pitchford, A.C. and Sarret, H.J., "Paving Asphalt Containing Chlorinated Polyethylene", U. S. Patent No 3,312,649, April, 1967.

19. Fogg, S.G. and Westerman, P.H., "Bituminous Compositions Containing a Chlorinated Polymer", U. S. Patent No 1,475,924, July, 1977.

20. Gaylord, N.G., "Maleation of Linear Low-Density Polyethylene by Reactive Processing", *Journal of Applied Polymer Science*, Vol. 44, 1992, pp. 1941-1949.

21. Masahiko, O., Japan Patent No. 7,730,546, 1977.

22. Biesenberger, J.A., *Reactive Extrusion-Principles and Practice*, Oxford University Press, New York, 1992, pp.55-65.

23. Singh, R.P., *Prog. Polymer Science*, Vol. 17, 1992, p. 251.

24. Kiyotada, N., Japan Patent No. 7,828,940, 1978.

25. Carraher, C.E. and J.A. Moore, *Modification of Polymers*. Plenum Press, New York, 1983, pp.171-190.

26. Gaylord, N.G., "High Density Polyethylene-g-Maleic Anhydride Preparation in Presence of Electron Donors", *Journal of Applied Polymer Science*, Vol, 38, 1989, pp. 359-371.

27. Qiu, Z.-Y., "Study of Asphalt and Polymer Modified Asphalt: Microstructure, Compatibility and Reinforcement Effect", Thesis, 1994, Louisiana State University.

28. Brown, S. F., Rowlett, R. D., and Boucher, J.L., "Highway Research: Shearing the Benefits", Proceedings, The United States Strategic Highway Research Program Conference, London, 1990.

29. Button, J., "Summary of Asphalt Additive Performance at Selected Sites", *Transportation Research Records*, Vol. 1342, 1992, pp. 67-75.

30. Gaylord, N.G., "Maleic Anhydride-Modified Polymers", U. S. Patent No 4,506,056, 1985.

31. Hogt, A., "Modification of Polypropylene with Maleic Anhydride". *SPE ANTEC'88 Preprints*, 1988, pp.1478-1480.

32. Cantor, K.M., "Improving Adhesion in Reinforced Polypropylene". *SPE ANTEC'93 Preprints*, 1993, pp. 1950-1953.

33. Kozel, T.H. and Kazmierczak, R.T. "A Rapid Fourier Transform Infrared (FTIR) Method for the Determination of grafted Maleate on Polyolefins", *SPE ANTEC'91 Preprints*, 1991, pp. 1570-1573.

34. Mohammad, L.N.. and Paul, H.R., "Evaluation of a New Indirect Tension Test for Determining the structural properties of Asphalt Mix", *Transportation Research Record*, Vol. 1417, 1993, pp. 58-63.

35. Mohammad, L.N. and Paul, H.R., "Evaluation of a New Indirect Tension Test Apparatus", *Transportation Research Record*, Vol. 1353, 1992, pp. 62-68.

36. Kim, Y.R., N. Kim, and N.P. Khosla, "Effects of Aggregate Type and Gradation on Fatigue and Permanent Deformation of Asphalt Concrete", ASTM STP 1147, Richard Meininger, Editor, American Society for Testing and Materials, Philadelphia, 1992, pp. 310-328.

37. Chai, Z., Shi, L., and Sheppard, R.N., "Microstructure of Solution-chlorinated Polyethylene by 13C Nuclear Magnetic Resonance", *Polymer*, Vol. 25, No. 3, 1984, pp. 369-374.

38. Chang, B.H., Zeigler, R., and Hiltner, A., "Chlorinated High-density Polyethylene. II. Solid State Structure", *Polym. Eng. Sci.*, Vol. 28, No. 18, 1988, pp. 1167-81.

39. Brandrup, J. and Immergut, E.H., *Polymer Handbook*, 2nd ed., 1975, V-14.

40. Gaylord, N.G. and Mehta, M., "Role of Homopolymerization in the Peroxide-Catalyzed Reaction of Maleic Anhydride and Polyethylene in the Absence of Solvent", *J. Poly. Sci. Poly. Lett. Ed.*, Vol. 20, 1982, pp. 481-486.

41. Gaylord, N.G., Mehta, M., and Mehta, R., "Degradation and Crosslinking of Ethylene-Propylene Copolymer Rubber on Reaction with Maleic Anhydride and/or Peroxides", *J .Appl. Poly. Sci*, Vol. 33, 1987, pp. 2549-2558.

42. Liu, N.C., Baker, W.E., and Russell, K.E., "Functionalization of Polyethylenes and Their Use in Reactive Blending", *J. Appl. Poly. Sci.*, Vol. 41, 1990, pp. 2285-2300.

43. Sathe, S. N., Rao, G. S. S, and Devi, S., "Grafting of Maleic Anhydride onto Polypropylene: Synthesis and Characterization", *J. Appl. Polym. Sci.*, Vol. 53, 1994, pp. 239-245.

44. Domszy, R.C., Alamo, R., Edwards, C.O., and Mandelkern, L.., "Thermoreversible Gelation and Crystallization of Homopolymers and Copolymers", *Macromolecules*, Vol. 19, 1986, pp. 310-325.

45. Negulescu, I.I., Yeh, P.-H., Qiu, Z.-Y., and Daly, W. H., "Analysis of Asphalt Cements by Differential Scanning Calorimetry", North American Thermal Analysis Society (NATAS), McLean, VA, 1997, pp. 764-773.

46. Petersen, J.C., "Chemical Composition of Asphalt as Related to Asphalt Durability, State of the Art", *Transportation Research Record*, Vol. 999, 1984, pp. 13-30.

47. Daly, W.H., Qiu(Chiu), Z.-Y., and Negulescu, I.I., "Preparation and Characterization of Asphalt-Modified Polyethylene Blends", *Transportation Research Record*, Vol. 1391, 1993, pp. 56-64.

48. Terrel, R.L. and J.A. Epps, *Using Additives and Modifiers in Hot Mix Asphalt*, National

Asphalt Pavement Association (NAPA): Riverdale, MD, 1989, p. 114.

This public document is published at a total cost of $1163.00. Two hundred and twenty five copies of this public document were published in this first printing at a cost of $757.00. The total cost of all printings of this document including reprints is $1163.00. This document was published by Louisiana State University, Graphic Services, 3555 River Road, Baton Rouge, Louisiana 70802, and Louisiana Transportation Research Center, to report and publish research findings for the Louisiana Transportation Research Center as required in R.S. 48:105. This material was duplicated in accordance with standards for printing by state agencies established pursuant to R.S. 43:31. Printing of this material was purchased in accordance with the provisions of Title 43 of the Louisiana Revised Statutes.